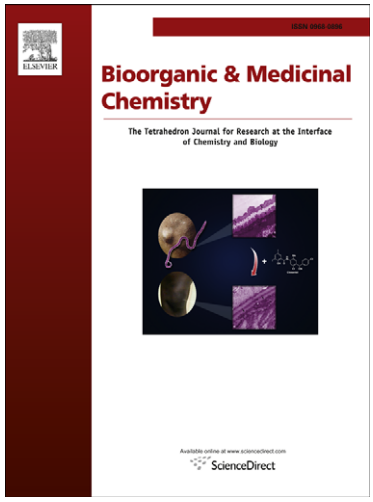

Lead identification of β-lactam and related imine inhibitors of the molecular chaperone heat shock protein 90

Niamh M. O'Boyle, Andrew J.S. Knox, Trevor P. Price, D. Clive Williams, Daniela M. Zisterer, David G. Lloyd, Mary J. Meegan

PII: S0968-0896(11)00682-1
DOI: 10.1016/j.bmc.2011.08.048
Reference: BMC 9462

To appear in: *Bioorganic & Medicinal Chemistry*

Received Date: 18 February 2011
Revised Date: 18 August 2011
Accepted Date: 19 August 2011

Please cite this article as: O'Boyle, N.M., Knox, A.J.S., Price, T.P., Williams, D.C., Zisterer, D.M., Lloyd, D.G., Meegan, M.J., Lead identification of β-lactam and related imine inhibitors of the molecular chaperone heat shock protein 90, *Bioorganic & Medicinal Chemistry* (2011), doi: 10.1016/j.bmc.2011.08.048

Lead identification of β-lactam and related imine inhibitors of the molecular chaperone heat shock protein 90

Niamh M. O'Boyle[1*], Andrew J.S. Knox[2], Trevor P. Price[2], D. Clive Williams[2], Daniela M. Zisterer[2], David G. Lloyd[3], Mary J. Meegan[1*]

[1]*School of Pharmacy and Pharmaceutical Sciences, Centre for Synthesis and Chemical Biology, Trinity College Dublin, Dublin 2, Ireland*

[2]*School of Biochemistry & Immunology, Trinity College Dublin, Dublin 2, Ireland*

[2]*Molecular Design Group, School of Biochemistry & Immunology, Trinity College Dublin, Dublin 2, Ireland*

*To whom correspondence should be addressed

*Corresponding authors. Dr. Niamh M. O'Boyle and Professor Mary J. Meegan, School of Pharmacy and Pharmaceutical Sciences, Centre for Synthesis and Chemical Biology, Trinity College Dublin, Dublin 2, Ireland.

Tel: +353-1-8962798; Fax: +353-1-8962793;

E-mail: oboyleni@tcd.ie; mmeegan@tcd.ie

Abstract

Heat shock protein 90 is an emerging target for oncology therapeutics. Inhibitors of this molecular chaperone, which is responsible for the maintenance of a number of oncogenic proteins, have shown promise in clinical trials and represent a new and exciting area in the treatment of cancer. Heat shock protein 90 inhibitors have huge structural diversity, and here we present the lead identification of novel inhibitors based on β-lactam and imine templates. β-Lactam **5** and imines **12** and **18** exhibit binding to heat shock protein 90-α with IC_{50} values of 5.6 μM, 14.5 μM and 22.1 μM respectively. The binding affinity displayed by these compounds positions them as lead compounds for the design of future inhibitors of heat shock protein 90 based on the β-lactam and imine templates.

Key words

Heat shock protein 90, Hsp90, β-lactam, azetidinone, imine, structure-activity relationship, anti-cancer

Abbreviations

17-AAG	17-Allylamino-17-demethoxygeldanamycin
17-DMAG	17-Dimethylaminoethylamino-17-demethoxygeldanamycin
DMF	Dimethylformamide
DMSO	Dimethylsulfoxide
GA	Geldanamycin
HIF	Hypoxia-inducable factor
HRMS	High Resolution Molecular Ion Determination
Hsp90	Heat shock protein 90
HTMA	Hexamethylenetetramine (hexamine)
IR	Infra Red

MTT	3-(4,5-Dimethylthiazol-2-yl)-2,5-diphenyltetrazolium bromide
NMR	Nuclear Magnetic Resonance
PBS	Phosphate buffered saline
TBDMS	Tertbutyldimethylchlorosilane
TMCS	Trimethylchlorosilane
TLC	Thin layer chromatography

Introduction

Heat shock protein 90 (Hsp90) is a molecular chaperone that has a diverse 'clientele' of proteins, many of which are signal transducers that have roles in cellular proliferation and survival pathways[1]. A significant number of these proteins are oncogenic in nature and include protein kinases ERBB2 and BRAF, mutant p53 and steroid hormone receptors (estrogen and androgen)[1, 2]. The ability of Hsp90 inhibition to affect many oncogenic signaling cascades simultaneously through inhibition of a single target is highly desirable and unique and marks it as an attractive target for cancer therapy[1].

Hsp90 consists of three flexibly linked domains. The N-terminal domain contains an unusual adenine-nucleotide-binding pocket known as the Bergerat fold[3]. An ATPase cycle is central to the chaperoning activity of Hsp90. Hsp90 inhibitors geldanamycin (**1a**, figure 1)[4], a related derivative, 7-allylaminogeldanamycin (17-AAG, **1b**)[5] and radicicol (**2**, figure 1)[6, 7] bind at this ATP-site, leading to diminished ATPase activity and preventing dissociation of client proteins from the Hsp90 complex[8]. Although radicicol has higher affinity for full-length homodimeric Hsp90 than geldanamycin, it has not progressed as far in terms of drug development. *In vitro* all three mediate the characteristic response to Hsp90 inhibition – depletion of client proteins and upregulation of heat shock proteins[6], but the presence of epoxy and unsaturated carbonyl groups in radicicol leads to inactivation *in vivo* by 1,6-Michael addition with thiol-derived nucleophiles[9].

Many small molecule inhibitors of Hsp90 have been reported[10]. High-throughput screening of a chemical library of 60,000 compounds identified the pyrazole based structure **3a** (figure 1) as a Hsp90 inhibitor[11]. This compound causes depletion of Hsp90

client proteins, induction of Hsp70, upregulation of heat shock proteins, growth arrest and apoptosis in cancer cells, although *in vivo* activity and toxicity have yet to be reported[1, 12]. The resorcinol ring mimics the substitution on the aromatic ring of radicicol (**2**, figure 1). Extensive structure-activity relationships have been determined for the pyrazole based Hsp90 ligands[13-15]. Other Hsp90 small-molecule inhibitors include many purine-based analogues including **3c**[16] and indazole **4** as the first reported compound to target both Hsp90 and tubulin (figure 1)[17]. At the end of 2010, thirteen Hsp90 inhibitors were reported to be in clinical trials, including 17-AAG **1b** and a related geldanamycin derivative, 17-DMAG (**1c**, figure 1)[18, 19]. Additional Hsp90 inhibitors for which structures have since been disclosed and which are not yet reported in reviews include Debio 0932 (formerly CUDC-305)[20], AT13387[21] and KW-2478[22].

The number of structurally diverse Hsp90 inhibitors in clinical trials indicates the ability of the Hsp90 ATP-binding site to accommodate a large variety of chemical structures. The pyrazole scaffold of **3a** is a small nitrogen-containing heterocyclic core, similar to a β-lactam nucleus, and we were interested in determining if the β-lactam scaffold was capable of acting as a template for Hsp90 inhibitors. The β-lactam ring scaffold is an established template for antibiotics[23], cholesterol absorption inhibitors[24] selective estrogen receptor modulators[17] and antiproliferative tubulin-binding antiproliferative agents[25, 26]. Herein, we report the synthesis and biochemical evaluation of a β-lactam based Hsp90 inhibitor **5** (figure 1) and related compounds, which was designed to contain similarly substituted aryl rings positioned at C-4 and N-1 to the aryl substituents at C-3 and C-4 of pyrazole **3a** (figures 1 and 2). The proposed compounds would add further structural diversity to the rapidly expanding field of small molecule Hsp90 inhibitors, with potential applications in the area of Hsp90 based therapeutics, and provide additional insights into the chemical scaffolds that can be accommodated in the Hsp90 N-terminal ATP-binding site.

Molecular modelling

Molecular modelling studies on the proposed Hsp90-binding β-lactam **5** were carried out to explore potential binding interactions with the N-terminal ATP-binding site of Hsp90. In addition, the synthetic imine precursors to β-lactam preparation were examined as they possess the necessary pharamacophore required for binding to the Hsp90 protein. Existing X-ray co-crystal structures of the Hsp90 N-terminal ATP-binding site with

ADP[3], geldanamycin (**1a**)[8], radicicol (**2**)[7], 17-DMAG (**1c**)[27] and small-molecule Hsp90 inhibitors pyrazole **3a**, **3b**[11, 28] and purine **3c**[16] (figure 1) provide insight into the requirements for binding to Hsp90. The binding pocket is of mixed hydrophobic and polar character, with approximately half of the 17 amino acids lining its interior being hydrophobic, a quarter polar and a quarter charged. Mutation of the Asp93 residue to asparagine abolishes Hsp90 function *in vivo*[7]. As the binding pocket becomes increasingly hydrophobic towards the bottom, Asp93 is the only charged residue in the deepest part of the binding pocket, along with one polar residue (Thr 184)[8]. Asp93 is conserved in all known Hsp90 homologs from 35 species[8]. These interactions are considered critical for binding of small molecule Hsp90 inhibitors.

Molecular docking studies show that β-lactam **5** (figure 1) is predicted to interact with the ATP-binding site of Hsp90 in a similar manner to both radicicol and the pyrazole class of small molecule inhibitors[7, 11]. Flexible alignment of **5** with pyrazole **3a** reveals a large degree of overlap between the resorcinol and benzodioxan rings but a slight offset of the nitrogen heterocycle itself (figure 2). When docked in the ATP-binding site of Hsp90, β-lactam **5** is seen to be orientated with the ethylresorcinol ring extended towards the bottom of the ATP-binding pocket, and the benzodioxane ring towards the top of the pocket and into solvent (figure 3). This is a similar binding conformation to radicicol and could be expected from the similar substitution pattern on the aromatic rings of the two compounds. The crucial interaction at the bottom of the binding pocket between a phenolic group on the β-lactam with Asp93 is present (figure 3). Interactions with Thr184 are also seen for **5**, mimicking key interactions of the endogenous adenine base and also the natural product ligands geldanamycin and radicicol. Nearing the top of the binding cavity, interactions with Lys112 are present amongst others. A 2D representation of these interactions is illustrated (figure 4)[29]. Interactions with Asp93 are common to all Hsp90 ligands and can be considered to be necessary for binding to Hsp90. β-Lactam compounds without the resorcinol hydroxyl groups, such as methoxy-containing derivatives **19** and **20**, are not predicted to interact with Asp93 and this is likely to account for the lack of binding affinity observed *in vitro*.

Imine **12**, the synthetic precursor to β-lactam **5** was also docked in the ATP-binding site on the N-terminal of Hsp90 as it also contains the required pharmacophore for Hsp90 binding (figures 5 and 6). The molecule is predicted to adopt a similar orientation to radicicol, with the two hydroxyl groups and the ethyl group penetrating deep into the

pocket and interacting with Asp93 and a conserved water molecule. The dioxane ring points towards the top of the binding pocket and binding is reinforced by strong hydrogen bonding interactions with Lys58 and Asn106 (figures 5 and 6). Interactions with Met98, Phe138, Lys58, Asp102, Ala55 and Ser52 are also predicted for the imine. These interactions are present for geldanamycin and other Hsp90 ligands and are identified as a common requirement of Hsp90 activity in a number of co-crystallised structures. On the basis of this molecular docking study, it would be expected that imine **12** would display Hsp90 binding affinity.

Chemistry

The 4-ethylresorcinol and 4-chlororesorcinol moieties are two of the most commonly seen ring systems in a broad range of Hsp90 inhibitors, including radicicol (**2**) and pyrazole **3a**[10, 12, 30]. In order to design β-lactams containing these aryl substitution patterns, the synthesis of appropriate aldehydes as precursors for the required imines was first carried out. It was also necessary to protect both hydroxyl groups of the resorcinol molecule prior to the β-lactam forming reactions. 4-Ethylresorcinol and 4-chlororesorcinol are commercially available. The formylation of 4-ethylresorcinol (**6b**) was achieved using a Vilsmeier-Haack reaction, utilising N,N-dimethylformamide and phosphorus oxychloride (scheme 1)[31]. The formylated product **7b** was obtained from **6b** in yields of up to 36%. ^{1}H NMR analysis shows an additional chemical shift at δ 9.91 ppm attributable to the aldehyde proton, there is disappearance of one aromatic signal and the remaining two aromatic protons appear as singlets at δ 6.39 and δ 7.34 ppm. IR spectroscopy analysis shows absorption at ν 1645.8 cm^{-1} due to the carbonyl group. The Vilsmeier-Haack reaction using phosphorous oxychloride and anhydrous dimethylformamide was unsuccessful for the formylation of 4-chlororesorcinol. The Duff reaction[32-34], using hexamethylenetetramine (hexamine) in acidic solution at room temperature did not result in formylation, whilst heating at 100˚C led to formylation at both the 2 and 6 positions of 4-chlororesorcinol (**6c**) to afford **7c**.

Benzyl protection of the resorcinol phenolic groups was achieved using benzyl bromide and potassium hydroxide to give the desired product (scheme 1). The phenolic groups of commercially available 2,4-dihydroxybenzaldehyde (**7a**) were protected by this method to prepare **8a** (scheme 1). The dibenzylprotected product **8b** was obtained in 90% yield from 5-ethyl-2,4-dihydroxybenzaldehyde **7b**. Use of the TBDMS group was also

investigated. This protecting group did not remain intact during Vilsmeier-Haack formylation. Silylation of aldehyde **7b** was attempted, resulting in protection of only one of the phenolic groups. This is thought to be due to intramolecular H-bonding between the aldehyde and phenolic groups on adjacent positions of the aromatic ring.

Hsp90 imine precursors **9** – **18** were obtained by condensation of the appropriately substituted aldehydes and amines (scheme 1). Yields for all products were over 85% with the exception of **18** (59%). The characteristic signal at approximately δ 8.70 – 8.85 ppm in the ^{1}H NMR spectra attributable to the imine proton was observed for all products.

The initial Hsp90-targeting β-lactams chosen for synthesis are unsubstituted at the 3-position of the azetidinone ring (compounds **19-25**). The Reformatsky reaction using microwave technology was employed to synthesise these compounds in low yields, by reaction of imines **9-18** with ethyl bromoacetate (scheme 2). All intermediate compounds **19** – **25** showed IR absorptions at approximately ν 1740 cm^{-1} confirming formation of the azetidin-2-one. The synthesis of an alternative structural example, compound **26,** was achieved containing a phenyl substituent at the 3-position of the β-lactam ring, as we wished to investigate the effect of the introduction of a larger substituent at the C-3 position. This analogue was obtained with exclusively *trans* geometry as evidenced by the coupling constant of 2.0 Hz between the protons at positions 3 and 4 of the β-lactam ring.

Benzyl protecting groups were removed from compounds **21** – **26** subsequent to the Reformatsky reaction by hydrogenation over a palladium catalyst leaving the β-lactam ring intact to form six different final products **5** and **27** – **31** (scheme 3). The substitutions on the N-1 aryl ring reflect the aryl substitution pattern observed for pyrazole analogues with the greatest Hsp90 activity previously reported in literature[11, 17, 28]. As discussed previously, the lead β-lactam compound **5** mimics the substitution pattern of the pyrazole **3a**. A number of analogues were designed to confirm that the two hydroxyl groups and the ethyl group of the resorcinol ring are essential for Hsp90 activity. β-Lactam **27** lacks an ethyl group, and compounds **19** and **20** substitute methoxy groups for the hydroxyls. Pyrazoles with either a 4-methoxyphenyl ring[28] or methylenedioxane[11] ring in place of the benzodioxane ring has been shown to have improved activity and the corresponding β-lactam analogues **28** and **29** were also

synthesised. Finally, β-lactam containing the trimethoxyphenyl ring found in the dual-acting inhibitor **4** was also prepared.

Biochemical Evaluation

The Hsp90 binding affinities of β-lactams **5, 27-31** (scheme 3) were first evaluated using a fluorescent displacement assay and Hsp90 recombinant human protein, based on their ability to compete with geldanamycin for Hsp90 binding[35]. Two imines, **12** and **18**, were also screened for activity as they possess the necessary pharmacophore for binding to Hsp90. Of the series of β-lactams evaluated, azetidinone **5** was the only compound to show a significant effect in the Hsp90α binding assay with an IC_{50} value of 5.63 μM (figure 7). The other seven analogues showed disappointing activity with IC_{50} values greater than 200 μM (table 1). Low activity was expected for β-lactams **19**, **20** and **27** as they were synthesised to confirm that the hydroxy and ethyl substituents of the resorcinol ring were necessary for activity. Analogues **19** and **20** replace the hydroxy groups of **5** with methoxy groups, and this substitution leads to marked decrease of Hsp90 binding ability. This is consistent with literature reports that the hydroxyl groups of the resorcinol ring are essential for hydrogen bonding interactions with the Hsp90 protein[13, 14]. Analogue **27**, with the hydroxyl groups of **5** intact but without the ethyl group, shows decreased activity compared to **5**, indicating that the ethyl group of **5** is also crucial for to Hsp90 binding activity. This pattern of activity was seen for radicicol and analogues, where analogues that lack the chloro substituent of radicicol at this position have substantially lower affinity for Hsp90[36]. The lack of binding affinity was not anticipated for β-lactam **29**, in which the benzodioxane ring of **5** is replaced with a 3,4-methylenedioxyphenyl moiety. This substitution leads to an over 40-fold reduction in activity. Similar substitution has been made in a purine series of compounds and did not result in decreased activity[11]. The monomethoxy ring at the N-1 position of β-lactam **28** and trimethoxy ring at the N-1 position of β-lactam **30** also did not result in any Hsp90 binding affinity. The substitutions at the N-1 position of the β-lactam ring are likely to be orientated out of the ATP-binding pocket and into solvent, not providing optimal binding compared to the benzodioxane ring of **5**. Imines **12** and **18** exhibited IC_{50} values of 14.49 μM and 22.08 μM respectively in the Hsp90 binding assay. A dose-response curve for **12** is shown alongside that of azetidinone **5** and 17-AAG in figure 7. These are the first reported imines with Hsp90 binding activity.

The antiproliferative activity of Hsp90 binding compounds has been evaluated in various cell lines including HCT116 colon cells[15, 28, 37], MCF-7 breast cancer cells[38-42], SKBr3 breast cancer cells[38, 41, 43, 44] and BT474 breast cancer cells[45]. In the present work

the antiproliferative effects of the imines and azetidinones synthesised was evaluated in human MCF-7 breast cancer cells (table 1). The most potent antiproliferative compound was dihydroxy analogue **27** with an IC_{50} value of 23.50 μM in MCF-7 cells. The only β-lactam that significantly inhibited Hsp90, **5**, displayed an IC_{50} value of 48.22 μM in MCF-cells. The two imines that showed inhibition of Hsp90, **12** and **18**, did not show antiproliferative activity in MCF-7 cells at concentrations up to 100 μM. The lack of correlation between the binding affinity of these compounds for Hsp90 and their antiproliferative activity warrants future evaluation of these compounds in a cell line such as the K562 chronic myelogenous leukaemia (CML), as a client protein Bcr-Abl is readily degraded in response to Hsp90 inhibition[46].

The "On Target" activity of the β-lactam Hsp90 inhibitor **5** as well as imine-scaffold compounds **12** and **15** was analysed by investigating their ability to bind to the Hsp90 ATP binding site and subsequently induce proteosomal degradation of the Hsp90 client protein, estrogen receptor alpha (ER-α). Human ER-α positive breast cancer cells, MCF-7, were treated with vehicle, compound **5**, **12**, **18** or a known Hsp90 inhibitor, 17-AAG, at indicated concentrations (figure 8). The positive control, 17-AAG, potently induces degradation of ER-α at concentrations as low as 1μM, in line with previous reports[17, 47]. Test compounds **5**, **12** and **18** were treated at concentrations between 50μM and 200μM, comparable to IC_{50} values for cell death induced by these compounds in MCF-7 cells (table 1). Results indicate that treatment with all three compounds induced degradation of ER-α in MCF-7 cells (figures 8A and 8B). In line with the binding displacement assay and cytotoxicity data, **5** was the most potent compound inducing partial degradation at 50μM and complete loss of ER-α expression with 100μM and 150μM incubations. These results indicate that the lead β-lactam compound **5** as well as imines **12** and **18** act as Hsp90 inhibitors.

Conclusion

Two novel templates for Hsp90 inhibitor design were identified. The first reported β-lactam and imine inhibitors of Hsp90 are described. β-Lactam compound **5** was designed to contain similarly substituted aryl rings positioned at C-4 and N-1 to the aryl substituents at C-3 and C-4 of pyrazole **3**, a known Hsp90 inhibitor as we wished to determine if the β-lactam scaffold was capable of acting as a template for providing the necessary interactions with the Hsp90 ATP-binding site. Molecular modelling studies

were used prospectively to examine proposed binding interactions for both β-lactam compound **5** and imine **12** in the ATP binding site of Hsp90. β-Lactam **5** displayed significant inhibition of Hsp90α with an IC_{50} of 5.63 μM and a moderate IC_{50} value of 48.22 μM in an antiproliferative assay using MCF-7 human breast cancer cells. Two imines, **12** and **18** (synthetic precursors of the β-lactams **5** and **29** respectively), were identified as having the required pharmacophore for Hsp90 binding and were also evaluated for Hsp90 binding activity. They displayed promising results with low micromolar inhibition of Hsp90α. β-Lactam **5**, as well as imines **12** and **18**, were demonstrated to induce proteosomal degradation of the Hsp90 client protein ERα. From our results showing the displacement of the N-terminal binding agent geldanamycin, together with the structural similarity of the compounds to the previously reported N-terminal binding agents, we can conclude that these β-lactams and imines bind at the N-terminal domain of Hsp90 rather than acting at the C-terminal domain in a manner that is similar to the novobiocin analogues. These results expand the range of known structural types accommodated by the ATP-binding site of Hsp90 and may contribute to the future use of Hsp90 directed therapeutics for the treatment of cancer. Future SAR work will aim to improve the antiproliferative activity and the physiochemical properties of the identified lead compounds.

Experimental section

Experimental note

All reagents were commercially available and were used without further purification unless otherwise indicated. IR spectra were recorded as thin films on NaCl plates or as KBr discs on a Perkin-Elmer Paragon 100 FT-IR spectrometer. ^{1}H and ^{13}C NMR spectra were obtained on a Bruker Avance DPX 400 instrument at 20^{o}C, 400.13MHz for ^{1}H spectra, 100.61MHz for ^{13}C spectra, in $CDCl_3$ or DMSO-d_6 (internal standard tetramethylsilane) by Dr. John O'Brien and Dr. Manuel Ruether in the School of Chemistry, Trinity College Dublin. High resolution accurate mass determinations for all final target compounds were obtained on a Micromass Time of Flight mass spectrometer (TOF) equipped with electrospray ionisation (ES) interface operated in the positive ion mode at the High Resolution Mass Spectrometry Laboratory by Dr. Martin Feeney in the School of Chemistry, Trinity College Dublin. Thin layer chromatography was performed using Merck Silica gel 60 TLC aluminium sheets with fluorescent indicator visualizing

with UV light at 254nm. Flash chromatography was carried out using standard silica gel 60 (230-400 mesh) obtained from Merck. Analytical high-performance liquid chromatography (HPLC) to determine the purity of the final compounds was performed using a Waters 2487 Dual Wavelength Absorbance detector, a Waters 1525 binary HPLC pump, a Waters In-Line Degasser AF and a Waters 717plus Autosampler. The column used was a Varian Pursuit XRs C18 reverse phase 150 x 4.6 mm chromatography column. Samples were detected using a wavelength of 254 nm. All samples were analysed using a mobile phase consisting of acetonitrile (70%): water (30%) over 10 min and a flow rate of 1 mL/min.

Procedure for Vilsmeir-Haack formylation of 4-ethylresorcinol

5-Ethyl-2,4-dihydroxybenzaldehyde (7b). Dimethylformamide (38.2 mmol) and phosphorous oxychloride (43.1 mmol) were mixed at 0˚C and stirred for 15 minutes before addition of 4-ethylbenzene-1,3-diol **6b** (14.5 mmol) dissolved in dimethylformamide (10 mL). The mixture was heated to 80˚C for eight hours. The reaction was quenched by the slow and careful addition of saturated aqueous sodium bicarbonate solution (150 mL) and was stirred overnight. The solution was extracted with CH_2Cl_2 (50 mL three times) and the combined organic layers were dried over Na_2SO_4. The pure product was isolated by flash column chromatography over silica gel (eluent: hexane:ethyl acetate gradient) and isolated as a white powder (yield 36.0%); Mp: 132ºC (lit. mp: 130-131ºC[48]); IR (KBr) ν_{max}: 1645.83 (-C=O), 3193.79 (broad, -OH) cm^{-1}; ^1H NMR (400 MHz, DMSO-d_6) δ 1.12 (t, 3H, CH_3), 2.49 (q, 2H, CH_2), 6.39 (s, 1H, ArH), 7.34 (s, 1H, ArH), 9.91 (s, 1H, CHO); ^{13}C NMR (400 MHz, DMSO-d_6) δ 13.92 (CH_3), 21.76 (CH_2), 101.79, 114.80, 122.98, 130.63, 161.44, 163.08 (ArC), 190.78 (C=O); HRMS: $C_9H_{10}O_3$ requires 167.0708; found 167.0711; Elemental analysis: Found: C, 64.99; H, 6.07; $C_9H_{10}O_3$ requires C, 65.05; H, 6.07%

5-Chloro-2,4-dihydroxyisophthalaldehyde (7c). To 4-chlorobenzene-1,3-diol (3 mmol) in trifluoroacetic acid (40 mL) was added HTMA (30 mmol, 10 equiv.). The mixture was heated to 100ºC for 30 minutes after which it was left to cool to room temperature. Water (60 mL) was carefully added followed by sodium bicarbonate (with vigorous stirring) until neutralised. Dichloromethane (100 mL) was added and the mixture was stirred for 2 hours at room temperature. The layers were separated, the

aqueous layer was extracted with dichloromethane:methanol (9:1, 100 mL) and the combined organic fractions were dried with anhydrous Na_2SO_4 and the solvent was removed *in vacuo*. The product was isolated as a white solid in 56.2% yield; ^{1}H NMR (400 MHz, $CDCl_3$) δ 7.29 (s, 1H, ArH), 7.79 (s, 1H, ArH), 9.73 (s, 1H, CHO), 10.41 (s, 1H, CHO), 12.42 (s, 1H, OH), 13.26 (s, 1H, OH); ^{13}C NMR (400 MHz, $CDCl_3$) δ 109.45, 113.15, 139.96, 164.44, 164.87 (ArC), 192.79 (C=O), 193.34 (C=O).

General procedure for dibenzyl protection of resorcinol derivatives. Benzyl bromide (0.11 mol) was added to a mixture of resorcinol derivative (0.045 mol) and potassium carbonate (0.11 mol) in acetonitrile (200 mL). The mixture was heated at reflux for 5 hours and stirred overnight at room temperature. The mixture was filtered and the solid filter cake was washed with CH_2Cl_2 (200 mL). The combined organic fractions were evaporated *in vacuo* to leave the product. The crude product was triturated with hexane and filtered to give the pure product.

2,4-Bisbenzyloxybenzaldehyde (8a) was prepared from 2,4-dihydroxybenzaldehyde **7a** and isolated as a white solid (98.0% yield); Mp: 85ºC (lit. mp: 85 - 86ºC[49]); IR (KBr) ν_{max}: 1677.88 cm^{-1} (-C=O); ^{1}H NMR (400 MHz, DMSO-d_6) δ 5.23 (s, 2H, CH_2), 5.29 (s, 2H, CH_2), 6.76 (d, 1H, J=8.8 Hz, ArH), 6.93 (s, 1H, ArH), 7.36 – 7.68 (m, 10H, ArH), 7.70 (d, 1H, J= 8.8 Hz, ArH), 10.25 (s, 1H, CHO); ^{13}C NMR (100 MHz, DMSO-d_6) δ 70.34 (CH_2), 70.38 (CH_2), 100.93, 108.15, 119.11, 128.03, 128.47, 128.63, 129.01, 129.04, 130.37, 136.67, 136.84, 162.87, 165.44 (ArC), 187.77 (C=O); HRMS: $C_{21}H_{18}O_3Na$ requires 341.1154; found: 341.1155 (M^++Na); Elemental analysis: Found: C, 78.89; H, 5.73; $C_{21}H_{18}O_3$ requires C, 79.22; H, 5.70%

2,4-Bisbenzyloxy-5-ethylbenzaldehyde (8b) was prepared from 5-ethyl-2,4-dihydroxybenzaldehyde (**7b**) according to the procedure above. The product was obtained as a white powder (yield 89.5%); Mp: 123ºC; IR (KBr) ν_{max}: 1663.00 cm^{-1} (-C=O); ^{1}H NMR (400 MHz, DMSO-d_6) δ 1.12 (t, 3H, CH_3), 2.54 (q, 2H, CH_2), 5.28 (s, 2H, CH_2), 5.30 (s, 2H, CH_2), 7.00 (s, 1H, ArH), 7.35 – 7.51 (m, 11H, ArH), 10.24 (s, 1H, CHO); ^{13}C NMR (100 MHz, DMSO-d_6) δ 13.90 (CH_3), 22.05 (CH_2), 69.86 (CH_2), 70.21 (CH_2), 98.33, 117.76, 125.06, 127.50, 127.55, 127.68, 128.06, 128.59, 128.63, 128.69, 129.29, 136.45, 161.34, 162.56 (ArC), 187.26 (C=O); HRMS: $C_{23}H_{22}O_3Na$

requires 369.1467; found: 369.1465 (M^++Na); Elemental analysis: Found: C, 79.74; H, 6.40; $C_{23}H_{22}O_3$ requires C, 78.83; H, 6.31%

General method for imine preparation

The appropriate amine (10 mmol) was heated at reflux with the appropriate aldehyde (10 mmol) in ethanol (50 mL) for 3 hours. The reaction mixture was cooled and then the solvent evaporated *in vacuo.* The resulting solid product was recrystallised from ethanol.

(2,3-Dihydrobenzo[1,4]dioxin-6-yl)(2,4-dimethoxybenzylidene)amine (9) was prepared from 2,3-dihydrobenzo[1,4]dioxin-6-ylamine and 2,4-dimethoxybenzaldehyde and isolated as a brown oil in 76.8% yield and was used in the subsequent reaction without further purification; IR (KBr) ν_{max}: 1609.48 cm^{-1} (-N=C-); ^{1}H NMR (400 MHz, $CDCl_3$) δ 3.86 (s, 3H, OCH_3), 3.87 (s, 3H, OCH_3), 4.26 (s, 4H, OCH_2CH_2O), 6.46 (s, 1H, ArH), 6.58 (d, 1H, J = 8.80 Hz, ArH), 6.81-6.89 (m, 3H, ArH), 8.15 (d, 1H, J = 8.76 Hz, ArH), 8.82 (s, 1H, HC=N); ^{13}C NMR (100 MHz, $CDCl_3$) δ 55.05, 55.09, 63.10, 64.24, 97.55, 97.92, 103.68, 105.16, 108.22, 109.25, 114.33, 116.89, 128.30, 143.18, 146.30, 154.30, 160.37, 163.13 (ArC); HRMS: $C_{17}H_{18}NO_4$ requires 300.1236; found 300.1239; (M^++H)

(2,3-Dihydrobenzo[1,4]dioxin-6-yl)(2,5-dimethoxybenzylidene)amine (10) was prepared from 2,3-dihydrobenzo[1,4]dioxin-6-ylamine and 2,5-dimethoxybenzaldehyde as a yellow solid in 25.0% yield; Mp: 69ºC; IR (KBr) ν_{max}: 1621.25 cm^{-1} (-N=C-); ^{1}H NMR (400 MHz, DMSO-d_6) δ 3.77 (s, 3H, OCH_3), 3.85 (s, 3H, OCH_3), 4.26 (s, 4H, OCH_2CH_2O), 6.78 – 6.90 (m, 3H, ArH), 7.10 (s, 2H, ArH), 7.49 (s, 1H, ArH), 8.78 (s, 1H, CH=N); ^{13}C NMR (100 MHz, DMSO-d_6) δ 55.93 (OCH_3), 57.74 (OCH_3), 64.52 (CH_2), 64.55 (CH_2), 110.01, 110.36, 114.04, 114.75, 117.85, 119.67, 124.88, 142.50, 144.06, 145.90 (ArC), 153.64 (C=N), 154.14, 154.21 (ArC); HRMS: $C_{17}H_{18}NO_4$ requires 300.123; found 300.1235, (M^++H); Elemental analysis: Found: C, 68.17; H, 5.72; N, 4.74; $C_{17}H_{17}NO_4$ requires C, 68.21; H, 5.72; N, 4.68%

4-[(2,3-Dihydrobenzo[1,4]dioxin-6-ylimino)methyl]benzene-1,3-diol (11) was prepared from 2,3-dihydrobenzo[1,4]dioxin-6-ylamine and 2,4-dihydroxybenzaldehyde as an orange solid in 95.4% yield; Mp: 144ºC; IR (KBr) ν_{max}: 1625.03 cm^{-1} (-N=C-); ^{1}H NMR (400 MHz, DMSO-d_6) δ 4.27 (s, 4H, OCH_2CH_2O), 6.28 (s, 1H, ArH), 6.40 (m, 1H, ArH), 6.85 – 6.95 (m, 3H, ArH), 7.40 (s, 1H, ArH), 8.75 (s, 1H, CH=N), 10.22

(broad s, 1H, OH), 13.62 (broad s, 1H, OH); ^{13}C NMR (100 MHz, DMSO-d_6) δ 64.54 (CH_2), 64.58 (CH_2), 102.81, 108.17, 109.56, 112.53, 115.10, 117.94, 134.67, 142.08, 142.61, 144.26 (ArC), 161.63 (C=N), 162.57, 163.27 (ArC); HRMS: $C_{15}H_{12}NO_4$ requires 270.0766; found 270.0776 (M^++H); Elemental analysis: Found: C, 66.14; H, 4.84; N, 5.24; $C_{15}H_{13}NO_4$ requires C, 66.41; H, 4.83; N, 5.16%

4-[(2,3-Dihydrobenzo[1,4]dioxin-6-ylimino)methyl]-6-ethylbenzene-1,3-diol (12) was prepared from 5-ethyl-2,4-dihydroxybenzaldehyde (**7b**) and 2,3-dihydrobenzo[*b*][1,4]dioxin-6-amine as orange powder in 87.0% yield; Mp: 181ºC; IR (KBr) ν_{max}: 1628.34 cm^{-1}, 1611.89 cm^{-1} (-N=C-), 3439.61 cm^{-1} (broad, OH); ^{1}H NMR (400 MHz, DMSO-d_6) δ 1.13 (t, 3H, CH_3), 2.46 – 2.51 (m, 2H, CH_2), 4.25 (s, 4H, OCH_2CH_2O), 6.34 (s, 1H, ArH), 6.84 – 6.92 (m, 3H, ArH), 7.26 (s, 1H, ArH), 8.71 (s, 1H, CH=N), 10.14 (broad s, 1H, OH), 13.35 (broad s, 1H, OH); ^{13}C NMR (100 MHz, DMSO-d_6) δ 14.20 (CH_3), 21.90 (CH_2), 64.07 (OCH_2CH_2O), 64.12 (OCH_2CH_2O), 102.03, 109.02, 111.72, 114.56, 117.46, 121.97, 132.61, 141.87, 142.04, 143.79 (ArC), 159.85 (C=N), 160.81, 161.17 (ArC); HRMS: $C_{17}H_{18}NO_4$ requires 300.1236; found 300.1237 (M^++H); Elemental analysis: Found: C, 67.85; H, 5.85; N, 4.50; $C_{17}H_{17}NO_4$ requires C, 68.21; H, 5.72; N, 4.68%

(2,4-Bisbenzyloxybenzylidene)(2,3-dihydrobenzo[1,4]dioxin-6-yl)amine (13) was prepared from 2,3-dihydrobenzo[1,4]dioxin-6-ylamine and 2,4-bisbenzyloxybenzaldehyde (**8a**) as a yellow powder in 90.5% yield; Mp: 144ºC; IR (KBr) ν_{max}: 1608.90 cm^{-1} (-N=C-); ^{1}H NMR (400 MHz, $CDCl_3$) δ 4.29 (s, 4H, OCH_2CH_2O), 5.12 – 5.14 (s, 4H, 2xCH_2), 6.63 (d, 1H, J=2.04 Hz, ArH), 6.68 – 6.71 (dd, 1H, ArH), 6.78 – 6.82 (m, 2H, ArH), 6.88 (d, 1H, J=8.56 Hz, ArH), 7.36 – 7.44 (m, 10H, ArH), 8.15 (d, 1H, J=8.52 Hz, ArH), 8.87 (s, 1H, CH=N); ^{13}C NMR (100 MHz, $CDCl_3$) δ 63.91 (CH_2), 63.98 (CH_2), 69.77 (CH_2), 70.01 (CH_2), 99.85, 106.52, 109.29, 114.28, 116.94, 126.90, 127.14, 127.67, 127.76, 127.87, 128.24, 128.28, 128.32, 128.50, 135.91, 141.30, 143.18 (ArC), 154.03 (C=N), 159.47, 162.18 (ArC); HRMS: $C_{29}H_{26}NO_4$ requires 452.1862; found 452.1865 (M^++H); Elemental analysis: Found: C, 76.89; H, 5.52; N, 2.99; $C_{29}H_{25}NO_4$ requires: C, 77.14; H, 5.58; N, 3.10%

(2,4-Bisbenzyloxy-5-ethylbenzylidene)(2,3-dihydrobenzo[1,4]dioxin-6-yl)amine (14) was prepared from 2,3-dihydrobenzo[1,4]dioxin-6-ylamine and 2,4-bisbenzyloxy-5-ethylbenzaldehyde (**8b**) as a yellow powder in 86.9% yield; Mp: 158ºC; IR (KBr) ν_{max}:

1625.71 cm^{-1} (-N=C-); ^{1}H NMR (400 MHz, $CDCl_3$) δ 1.23 – 1.27 (t, 3H, CH_3), 2.64 – 2.70 (m, 2H, CH_2), 4.30 (s, 4H, OCH_2CH_2O), 5.14 (s, 4H, 2xCH_2), 6.58 (s, 1H, ArH), 6.82 – 6.86 (m, 2H, ArH), 6.91 (d, 1H, J=8.52 Hz, ArH), 7.13 (s, 1H, ArH), 7.35 – 7.39 (m, 10H, ArH), 8.50 (s, 1H, CH=N); ^{13}C NMR (100 MHz, $CDCl_3$) δ 13.80 (CH_3), 22.18 (CH_2), 63.94 (CH_3), 63.97 (CH_3), 69.45 (CH_3), 99.73, 109.03, 111.89, 113.99, 117.26, 123.80, 126.71, 127.51, 128.16, 131.27, 136.22, 141.91, 143.49 (ArC), 159.64 (C=N), 160.19, 161.73 (ArC); HRMS: $C_{31}H_{30}NO_4$ requires 480.2175; found 480.2185 (M^++H); Elemental analysis: Found: C, 77.36; H, 6.11; N, 2.96; $C_{31}H_{29}NO_4$ requires C, 77.64; H, 6.10; N, 2.92%

Benzo[1,3]dioxol-5-yl(2,4-bisbenzyloxy-5-ethylbenzylidene)amine (15) was prepared from benzo[1,3]dioxol-5-ylamine and 2,4-bisbenzyloxy-5-ethylbenzaldehyde (**8b**) as a brown powder in 87.8% yield; Mp: 129ºC; IR (KBr) ν_{max}: 1611.89 cm^{-1} (-N=C-); ^{1}H NMR (400 MHz, $CDCl_3$) δ 1.26 (t, 3H, CH_3), 2.68 – 2.73 (m, 2H, CH_2), 5.11 (s, 4H, 2xCH_2), 5.99 (s, 2H, OCH_2O), 6.55 (s, 1H, ArH), 6.81 (s, 1H, ArH), 6.81 – 6.84 (m, 2H, ArH), 7.42 – 7.44 (m, 10H, ArH), 7.98 (s, 1H, ArH), 8.85 (s, 1H, CH=N); ^{13}C NMR (100 MHz, $CDCl_3$) δ 13.94 (CH_3), 22.45 (CH_2), 69.54 (CH_2), 70.57 (CH_2), 97.22, 100.76 (OCH_2O), 101.60, 107.82, 114.27, 117.37, 125.94, 126.60, 126.81, 126.88, 127.22, 127.56, 127.68, 128.22, 128.27, 136.22, 136.26, 145.02, 147.64 (ArC), 154.21 (C=N), 157.97, 159.64 (ArC); HRMS: $C_{30}H_{28}NO_4$ requires 466.2018; found 466.2018 (M^++H); Elemental analysis: Found: C, 76.38; H, 5.83; N, 2.93; $C_{30}H_{27}NO_4$ requires C, 77.40; H, 5.85; N, 3.01%

(2,4-Bisbenzyloxy-5-ethylbenzylidene)(3,4,5-trimethoxyphenyl)amine (16) was prepared from 3,4,5-trimethoxyaniline and 2,4-bisbenzyloxy-5-ethylbenzaldehyde (**8b**) as pale yellow flakes in 84.5% yield; Mp: 129ºC; IR (KBr) ν_{max}: 1607.16 cm^{-1} (-N=C-); ^{1}H NMR (400 MHz, $CDCl_3$) δ 1.25 (t, 3H, CH_3), 2.65 – 2.73 (m, 2H, CH_2), 3.90 (m, 9H, 3xOCH_3), 5.12 (s, 4H, 2xCH_2), 5.96 (s, 1H, ArH), 6.45 – 6.56 (m, 3H, ArH), 7.36 – 7.43 (m, 11H, ArH), 8.90 (s, 1H, CH=N); ^{13}C NMR (100 MHz, $CDCl_3$) δ 13.90 (CH_3), 22.44 (CH_2), 55.46 (OCH_3), 55.62 (OCH_3), 60.59 (OCH_3), 69.58 (CH_2), 70.57 (CH_2), 92.13, 97.17, 97.79, 126.61, 126.81, 127.61, 127.72, 127.85, 128.04, 128.24, 128.31, 136.18, 153.01 (ArC), 155.19 (C=N); HRMS: $C_{32}H_{34}NO_5$ requires 512.2437; found 512.2438 (M^++H); Elemental analysis: Found: C, 74.82; H, 6.44; N, 2.65; $C_{32}H_{33}NO_5$ requires C, 75.12; H, 6.50; N, 2.74%

(2,4-Bisbenzyloxy-5-ethylbenzylidene)(4-methoxyphenyl)amine (17) was prepared from 4-methoxyphenylamine and 2,4-bisbenzyloxy-5-ethylbenzaldehyde (**8b**) as a yellow powder in 90.5% yield; Mp: 139-140ºC; IR (KBr) ν_{max}: 1609.00 cm^{-1} (-N=C-); ^{1}H NMR (400 MHz, $CDCl_3$) δ 1.27 (t, 3H, CH_3), 2.68 – 2.74 (q, 2H, CH_2), 3.87 (s, 3H, OCH_3), 5.11 – 5.13 (s, 4H, 2xCH_2), 6.55 (s, 1H, ArH), 6.94 (m, 2H, ArH), 7.23 – 7.44 (m, 13H, ArH), 8.89 (s, 1H, CH=N); ^{13}C NMR (100 MHz, $CDCl_3$) δ 13.93 (CH_3), 22.45 (CH_2), 55.05 (OCH_3), 69.58 (CH_2), 70.60 (CH_2), 97.21 113.85, 114.34, 115.98, 121.77, 126.60, 126.81, 126.88, 127.58, 127.69, 127.75, 127.85, 128.04, 128.23, 128.26, 128.30, 136.21 (ArC), 153.95 (C=N), 161.12, 162.30 (ArC); HRMS: $C_{30}H_{30}NO_3$ requires 452.2226; found 452.2217 (M^++H); Elemental analysis: Found: C, 79.72; H, 6.47; N, 3.32; $C_{30}H_{29}NO_3$ requires C, 79.80; H, 6.47; N, 3.10%

4-((Benzo[d][1,3]dioxol-5-ylimino)methyl)-6-ethylbenzene-1,3-diol (18) was prepared from 5-ethyl-2,4-dihydroxybenzaldehyde (**7b**) and benzo[d][1,3]dioxol-5-amine as a green powder in 59.6% yield; Mp: 176ºC; IR (KBr) ν_{max}: 1633.59 cm^{-1}, 1610.87 cm^{-1} (-N=C-); ^{1}H NMR (400 MHz, DMSO-d_6) δ 1.13 (t, 3H, CH_3), 2.45 – 2.51 (m, 2H, CH_2), 6.06 (s, 2H, OCH_2O), 6.34 (s, 1H, ArH), 6.83 (d, 1H, J=2.24 Hz, ArH), 6.94 (d, 1H, J=8.28 Hz, ArH), 7.08 (d, 1H, J=2 Hz, ArH), 7.25 (s, 1H, ArH), 8.73 (s, 1H, CH=N), 10.18 (s, 1H, OH), 13.28 (s, 1H, OH); ^{13}C NMR (100 MHz, DMSO-d_6) δ 14.67 (CH_3), 22.35 (CH_2), 101.51, 101.89 (CH_2), 102.49, 108.91, 112.15, 115.97, 122.46, 133.06, 143.32, 146.17, 148.68, 160.33 (ArC), 161.15 (C=N), 161.56 (ArC); HRMS: $C_{16}H_{16}NO_4$ requires 286.1079; found 286.1075 (M^++H); Elemental analysis: Found: C, 66.52; H, 5.32; N, 4.94; $C_{16}H_{15}NO_4$ requires C, 67.36; H, 5.30; N, 4.91%

General method for synthesis of azetidinones 19 - 26

Zinc powder (0.927g, 15 mmol) was activated using trimethylchlorosilane (0.65 mL, 5 mmol) in anhydrous benzene (5 mL) by heating for 15 minutes at 40°C and subsequently for 2 minutes at 100°C in a microwave. After cooling, the appropriately substituted imine (10 mmol) and substituted ethylbromoacetate (12 mmol) were added to the reaction vessel and the mixture was refluxed in the microwave for 30 minutes at 100°C. The reaction mixture was filtered through Celite to remove the zinc catalyst and then diluted with dichloromethane (50 mL). This solution was washed with saturated ammonium chloride solution (20 mL) and 25% ammonium hydroxide (20 mL), and then with dilute HCl (40 mL), followed by water (40 mL). The organic phase was dried over

anhydrous sodium sulfate and the solvent was removed *in vacuo*. The pure product was isolated by flash column chromatography over silica gel (eluent: hexane: ethyl acetate gradient).

1-(2,3-Dihydrobenzo[1,4]dioxin-6-yl)-4-(2,5-dimethoxyphenyl)azetidin-2-one (19) was prepared by reaction of (2,3-dihydrobenzo[1,4]dioxin-6-yl)(2,5-dimethoxy-benzylidene)amine (**10**) and ethyl 2-bromoacetate in 13.2% yield as an orange powder; melting point: 164ºC; purity: 98.2%; IR (NaCl film) ν_{max}: 1746.30 cm^{-1} (C=O, β-lactam); ^{1}H NMR (400 MHz, $CDCl_3$) δ 2.85 – 2.90 (dd, 1H, H_3), 3.49 – 3.54 (m, 1H, H_3), 3.71 (s, 3H, OCH_3), 3.86 (s, 3H, OCH_3), 4.23 (s, 4H, OCH_2CH_2O), 5.28 – 5.31 (m, 1H, H_4), 6.76 – 6.88 (m, 6H, ArH); ^{13}C NMR (100 MHz, $CDCl_3$) δ 45.27 (C_3, CH_2), 48.41 (C_4), 55.27 (OCH_3), 55.53 (OCH_3), 63.75 (CH_2), 63.99 (CH_2), 105.74, 109.90, 111.14, 111.99, 112.81, 116.98, 126.78, 131.60, 139.53, 143.13, 150.75, 153.35 (ArC), 164.17 (C=O); HRMS: $C_{19}H_{20}NO_5$ requires 342.1341; found 342.1356 (M^++H)

1-(2,3-Dihydrobenzo[1,4]dioxin-6-yl)-4-(2,4-dimethoxyphenyl)azetidin-2-one (20) was prepared from (2,3-dihydrobenzo[1,4]dioxin-6-yl)(2,4-dimethoxy-benzylidene)amine (**9**) and ethyl 2-bromoacetate in 2.0% yield as a yellow oil; purity: 96.1%; IR (NaCl film) ν_{max}: 1744.56 cm^{-1} (C=O, β-lactam); ^{1}H NMR (400 MHz, $CDCl_3$) δ 2.85 – 2.89 (dd, 1H, H_3), 3.45 – 3.50 (m, 1H, H_3), 3.81 (s, 3H, OCH_3), 3.87 (s, 3H, OCH_3), 4.21 (s, 4H, OCH_2CH_2O), 5.23 – 5.25 (m, 1H, H_4), 6.44 – 6.50 (m, 2H, ArH), 6.75 (d, 1H, J=9.56 Hz, ArH), 6.84 – 6.87 (m, 2H, ArH), 7.13 (d, 1H, J=8.56 Hz, ArH); ^{13}C NMR (100 MHz, $CDCl_3$) δ 45.28 (C_3), 48.40 (C_4), 54.94 (OCH_3), 55.03 (OCH_3), 63.75 (CH_2), 64.00 (CH_2), 98.21, 103.96, 105.73, 109.93, 116.93, 117.85, 126.70, 131.71, 139.43, 143.10, 157.73, 160.27 (ArC), 164.42 (C=O); HRMS: $C_{19}H_{20}NO_5$ requires 342.1341; found 342.1331 (M^++H)

4-(2,4-Bisbenzyloxyphenyl)-1-(2,3-dihydrobenzo[1,4]dioxin-6-yl)azetidin-2-one (21) was prepared from (2,4-bisbenzyloxy-benzylidene)(2,3-dihydrobenzo[1,4]dioxin-6-yl)amine (**13**) and ethyl 2-bromoacetate in 17.9% yield as a brown gel; purity: 99.3%; IR (NaCl film) ν_{max}: 1745.51 cm^{-1} (C=O, β-lactam); ^{1}H NMR (400 MHz, $CDCl_3$) δ 2.87 – 2.92 (dd, 1H, H_3), 3.44 – 3.49 (dd, 1H, H_3), 4.22 (s, 4H, OCH_2CH_2O), 5.03 (s, 2H, CH_2), 5.11 (s, 2H, CH_2), 5.29 – 5.31 (m, 1H, H_4), 6.54 – 6.56 (m, 1H, ArH), 6.67 (s, 1H, ArH), 6.76 – 6.91 (m, 4H, ArH), 7.29 – 7.47 (m, 10H, ArH); ^{13}C NMR (100 MHz, $CDCl_3$) δ 45.33 (C_3), 48.36 (C_4), 63.76 (CH_3), 63.83 (CH_3), 69.82 (CH_3), 100.32, 105.46, 105.76,

109.91, 116.95, 118.58, 126.74, 126.93, 126.97, 127.10, 127.12, 127.15, 127.69, 127.72, 128.17, 128.22, 128.25, 131.71, 136.02, 136.20, 139.46, 143.15, 156.74, 159.37 (ArC), 164.28 (C=O); HRMS: $C_{31}H_{27}NO_5Na$ requires 516.1787; found 516.1792 (M^++H)

4-(2,4-Bisbenzyloxy-5-ethylphenyl)-1-(2,3-dihydrobenzo[1,4]dioxin-6-yl)azetidin-2-one (22) was prepared from (2,4-bisbenzyloxy-5-ethylbenzylidene)(2,3-dihydrobenzo[1,4]dioxin-6-yl)amine (**14**) and ethyl 2-bromoacetate in 5.6% yield as a brown gel and was deprotected to prepare **5** without further characterisation; HRMS: $C_{33}H_{31}NO_5Na$ requires 544.2100; found 544.2109 (M^++Na)

4-(2,4-bis(Benzyloxy)-5-ethylphenyl)-1-(4-methoxyphenyl)azetidin-2-one (23) was prepared from (2,4-bisbenzyloxy-5-ethylbenzylidene)(4-methoxyphenyl)amine (**17**) and ethyl 2-bromoacetate in 4.5% yield as a yellow solid; purity: 94.1%; IR (NaCl film) ν_{max}: 1727.60 cm^{-1} (C=O, β-lactam); ^{1}H NMR (400 MHz, DMSO-d_6) δ 1.02 – 1.06 (t, 3H, CH_3), 2.55 – 2.61 (m, 2H, CH_2), 2.88 – 2.92 (dd, 1H, H_3), 3.45 (m, 3H, OCH_3), 4.36 – 4.39 (m, 1H, H_3), 5.06 – 5.25 (m, 4H, 2xCH_2), 5.31 (m, 1H, H_4), 6.87 (m, 2H, ArH), 6.92 (s, 1H, ArH), 7.01 (s, 1H, ArH), 7.13 (m, 2H, ArH), 7.40 – 7.45 (m, 10H, ArH); ^{13}C NMR (100 MHz, DMSO-d_6) δ 14.70 (CH_3), 22.61 (CH_2), 45.21 (C_3), 48.73 (C_4), (OCH_3), 69.86 (CH_2), 70.34 (CH_2), 99.33, 114.63, 117.76, 117.90, 124.66, 127.31, 127.71, 127.96, 128.12, 128.17, 128.79, 128.82, 131.76, 137.29, 137.52, 155.51, 155.58, 156.83 (ArC), 164.43 (C=O); HRMS: $C_{32}H_{31}NO_4Na$ requires 516.2151; found 516.2156 (M^++Na)

1-Benzo[1,3]dioxol-5-yl-4-(2,4-bisbenzyloxy-5-ethylphenyl)azetidin-2-one (24) was prepared from benzo[1,3]dioxol-5-yl-(2,4-bisbenzyloxy-5-ethylbenzylidene)amine (**15**) and ethyl 2-bromoacetate in 6.2% yield as a brown gel; purity: 87.3%; IR (NaCl film) ν_{max}: 1738.89 cm^{-1} (C=O, β-lactam); ^{1}H NMR (400 MHz, $CDCl_3$) δ 1.13 (t, 3H, CH_3), 2.55 – 2.65 (m, 2H, CH_2), 2.92 – 2.96 (dd, 1H, H_3), 3.43 – 3.48 (m, 1H, H_3), 5.07 (m, 4H, 2xCH_2), 5.30 – 5.32 (m, 1H, H_4), 5.93 (s, 2H, OCH_2O), 6.60 (s, 1H, ArH), 6.68 (s, 2H, ArH), 7.03 – 7.07 (m, 2H, ArH), 7.36 – 7.44 (m, 10H, ArH); ^{13}C NMR (100 MHz, $CDCl_3$) δ 14.02 (CH_3), 22.37 (CH_2), 45.23 (C_3), 48.64 (C_4), 69.75 (CH_2), 70.36 (CH_2), 97.82, 99.00, 100.64 (OCH_2O), 107.75, 109.01, 125.48, 126.43, 126.62, 126.97, 127.47, 127.73, 128.17, 128.25, 132.41, 136.27, 136.63, 143.18, 147.32, 154.73, 156.54 (ArC), 164.41 (C=O); HRMS: $C_{32}H_{29}NO_5Na$ requires 530.1943; found 530.1953 (M^++Na)

4-(2,4-Bisbenzyloxy-5-ethylphenyl)-1-(3,4,5-trimethoxyphenyl)azetidin-2-one (25) was prepared from (2,4-bisbenzyloxy-5-ethylbenzylidene)(3,4,5-trimethoxyphenyl)amine (**16**) and ethyl 2-bromoacetate in 8.7% yield as a brown oil; purity: 98.8%; IR (NaCl film) ν_{max}: 1746.84 cm^{-1} (C=O, β-lactam); ^1H NMR (400 MHz, $CDCl_3$) δ 1.14 (t, 3H, CH_3), 2.56 – 2.66 (m, 2H, CH_2), 3.03 – 3.07 (d, 1H, H_3), 3.44 – 3.50 (dd, 1H, H_3), 3.74 (s, 3H, OCH_3), 3.89 (s, 6H, 2xOCH_3), 5.04 - 5.07 (m, 4H, 2xCH_2), 5.32 – 5.33 (d, 1H, J = 4.48 Hz, H_4), 6.59 (d, 3H, J = 11.04 Hz), 7.09 (s, 1H), 7.38 – 7.42 (m, 10H); ^{13}C NMR (100 MHz, $CDCl_3$) δ 14.14 (CH_3), 22.36 (CH_2), 44.92 (C_3), 48.74 (C_4), 55.52 (OCH_3), 60.51 (OCH_3), 69.70 (CH_2), 70.32 (CH_2), 93.96, 97.71, 117.10, 125.61, 126.60, 126.80, 126.99, 127.50, 127.76, 128.17, 128.25, 133.93, 136.13, 136.51, 152.94, 154.83 (ArC), 164.72 (C=O); HRMS: $C_{34}H_{35}NO_6Na$ requires 576.2362; found 576.2357 (M^++Na)

4-(2,4-Bisbenzyloxy-5-ethylphenyl)-1-(2,3-dihydrobenzo[1,4]dioxin-6-yl)-3-phenyl-azetidin-2-one (26) was obtained from (2,4-bisbenzyloxy-5-ethylbenzylidene)(2,3-dihydrobenzo[1,4]dioxin-6-yl)amine (**14**) and ethyl 2-bromo-2-phenylacetate as an orange oil in 3.3% yield; IR (NaCl film) ν_{max}: 1720.90 cm^{-1} (C=O, β-lactam); ^1H NMR (400 MHz, $CDCl_3$) δ 1.13 (t, 3H, CH_3), 2.58 – 2.63 (m, 2H, CH_2), 4.24 (s, 4H, OCH_2CH_2O), 4.29 (d, 1H, J=2 Hz, H_3), 5.03 (s, 2H, CH_2), 5.08 (s, 2H, CH_2), 5.35 (d, 1H, J=2 Hz, H_4), 6.61 (s, 1H, ArH), 6.78 (s, 1H, ArH), 6.98 (m, 1H, ArH), 7.09 (s, 1H, ArH), 7.16 (s, 1H, ArH), 7.29 – 7.44 (m, 15H, ArH); ^{13}C NMR (100 MHz, $CDCl_3$) δ 13.83 (CH_3), 21.90 (CH_2), 43.38 (C_3), 50.00 (C_4) 63.78, 63.92, 63.98, 69.84 (CH_2),100.08, 106.24, 110.35, 116.93, 126.77, 127.17, 128.06, 128.26, 131.33, 134.83, 135.94, 139.61, 143.11, 154.93 (ArC), 165.55 (C=O); HRMS: $C_{39}H_{34}NO_5$ requires 596.2436; found 596.2278 (M^+-H)

General procedure for preparation of β-lactams 5 and 27 – 31

The benzyl-protected compound (2 mmol) was dissolved in ethanol: ethyl acetate (50 mL; 1:1 mixture) and hydrogenated over 1.2g of 10 % palladium on carbon until the debenzylation was complete on TLC. The catalyst was filtered, the solvent was removed under vacuum and the product was isolated by flash column chromatography over silica gel (eluent: hexane: ethyl acetate gradient).

1-(2,3-Dihydrobenzo[1,4]dioxin-6-yl)-4-(5-ethyl-2,4-dihydroxyphenyl)azetidin-2-one (5) was prepared from 4-(2,4-bisbenzyloxy-5-ethylphenyl)-1-(2,3-

dihydrobenzo[1,4]dioxin-6-yl)azetidin-2-one (**22**) in 13.2% yield as a brown oil (purity: 97.4%); IR (NaCl film) ν_{max}: 1701.08 cm^{-1} (C=O, β-lactam); ^{1}H NMR (400 MHz, DMSO-d_6) δ 1.02 (t, 3H, CH_3), 2.40 (m, 2H, CH_2), 2.93 – 2.96 (dd, 1H, H_3), 3.37 – 3.41 (dd, 1H, H_3), 4.16 – 4.21 (m, 4H, OCH_2CH_2O), 5.12 – 5.13 (m, 1H, H_4), 6.37 (s, 1H, ArH), 6.76 (m, 2H, ArH), 6.87 (s, 1H, ArH), 7.32 (s, 1H, ArH), 9.21 (s, 1H, OH), 9.40 (s, 1H, OH); ^{13}C NMR (100 MHz, DMSO-d_6) δ 14.87 (CH_3), 21.07 (CH_2), 44.69 (C_3), 49.13 (C_4), 64.16 (CH_2), 64.53 (CH_2), 102.83, 105.42, 109.89, 113.63, 117.51, 121.41, 127.80, 132.38, 139.64, 143.55, 154.56, 155.77 (ArC), 164.90 (C=O); HRMS: $C_{19}H_{18}NO_5$ requires 340.1185; found 340.1187 (M^++H)

1-(2,3-Dihydrobenzo[1,4]dioxin-6-yl)-4-(2,4-dihydroxyphenyl)azetidin-2-one (27) was prepared from 4-(2,4-bisbenzyloxyphenyl)-1-(2,3-dihydrobenzo[1,4]dioxin-6-yl)azetidin-2-one (**21**) in 17.6% yield as an yellow powder; melting point: 166ºC; purity: 97.3%; IR (NaCl film) ν_{max}: 1712.93 cm^{-1} (C=O, β-lactam); ^{1}H NMR (400 MHz, DMSO-d_6) δ 2.88 – 2.92 (dd, 1H, H_3, J=17.08 Hz, J= 12.52 Hz), 3.35 – 3.43 (dd, 1H, H_3, J=20.56 Hz, J=9.04 Hz), 4.17 (m, 4H, OCH_2CH_2O), 5.13 – 5.15 (dd, 1H, H_4, J=8.04 Hz, J=2.88 Hz), 6.18 – 6.21 (m, 1H, ArH), 6.30 (m, 1H), 6.70 – 6.76 (m, 3H, ArH), 6.96 (d, 1H, J=8.56 Hz, ArH), 9.35 (s, 1H, OH), 9.68 (s, 1H, OH); ^{13}C NMR (100 MHz, DMSO-d_6) δ 44.48 (C_3), 48.61 (C_4), 63.82 (OCH_2CH_2O), 64.20 (OCH_2CH_2O), 102.54, 105.07, 106.77, 109.52, 113.89, 117.24, 128.06, 131.91, 143.24, 156.46, 158.13 (ArC), 164.46 (C=O); HRMS: $C_{17}H_{16}NO_5$ requires 314.1028; found 314.1020 (M^++H)

4-(5-Ethyl-2,4-dihydroxyphenyl)-1-(4-methoxyphenyl)azetidin-2-one (28) was prepared from 4-(2,4-bisbenzyloxyphenyl)-1-(4-methoxyphenyl)azetidin-2-one (**23**) as a yellow powder in 26.9% yield; purity: 90.4 %; IR (KBr) ν_{max}: 1732.59 cm^{-1} (C=O, β-lactam); ^{1}H NMR (400 MHz, DMSO-d_6) δ 0.98 (t, 3H, CH_3), 2.31- 2.35 (m, 2H, CH_2), 2.89 – 2.94 (m, 1H, H_3), 3.36 – 3.41 (m, 1H, H_3), 3.67 (s, 3H, OCH_3), 5.13 – 5.15 (dd, 1H, H_4), 6.34 (s, 1H, ArH), 6.84 (d, 3H, ArH), 7.16 (d, 2H, ArH), 9.21 (s, 1H, OH), 9.40 (s, 1H, OH); ^{13}C NMR (100 MHz, DMSO-d_6) δ 14.55 (CH_3), 22.14 (CH_2), 44.48 (C_3), 48.79 (C_4), 55.19 (OCH_3), 102.52, 113.46, 114.25, 117.52, 121.00, 127.38, 131.65, 154.21, 155.08, 155.39 (ArC), 164.42 (C=O); HRMS: $C_{18}H_{19}NO_4Na$ requires 336.1212; found 336.1207 (M^++Na)

1-Benzo[1,3]dioxol-5-yl-4-(5-ethyl-2,4-dihydroxyphenyl)azetidin-2-one (29) was prepared from 1-benzo[1,3]dioxol-5-yl-4-(2,4-bisbenzyloxy-5-ethylphenyl)azetidin-2-

one (**24**) as a brown powder in 44.6% yield; purity: 100%; IR (NaCl film) ν_{max}: 1720.37 cm^{-1} (C=O, β-lactam); ^{1}H NMR (400 MHz, DMSO-d_6) δ 1.01 (t, 3H, CH_3), 2.34 – 2.40 (m, 2H, CH_2), 2.94 – 2.98 (dd, 1H, H_3), 3.37 – 3.43 (dd, 1H, H_3), 5.13 – 5.15 (dd, 1H, H_4), 5.94 – 5.97 (m, 2H, OCH_2O), 6.36 (s, 1H, ArH), 6.65 – 6.68 (m, 1H, ArH), 6.84 – 6.89 (m, 3H, ArH), 9.26 (s, 1H, OH), 9.46 (s, 1H, OH); ^{13}C NMR (100 MHz, DMSO-d_6) δ 15.04 (CH_3), 22.62 (CH_2), 44.78 (C_3), 49.63 (C_4), 98.77, 101.49 (CH_2), 102.98, 108.87, 109.34, 113.64, 121.57, 128.03, 133.24, 143.34, 147.75, 154.72, 155.96 (ArC), 165.12 (C=O); HRMS: $C_{18}H_{17}NO_5Na$ requires 350.1004; found 350.1010 (M^++Na)

4-(5-Ethyl-2,4-dihydroxyphenyl)-1-(3,4,5-trimethoxyphenyl)azetidin-2-one (30) was prepared from 4-(2,4-bisbenzyloxy-5-ethylphenyl)-1-(3,4,5-trimethoxyphenyl)azetidin-2-one (**25**) in 6.2% yield as a white powder; purity: 96.1%; Melting point: 114°C; IR (KBr) ν_{max}: 1714.00 cm^{-1} (C=O, β-lactam); ^{1}H NMR (400 MHz, DMSO-d_6) δ 1.03 (t, 3H, CH_3), 2.34 – 2.42 (m, 2H, CH_2), 3.10 – 3.14 (dd, 1H, H_3), 3.56 (s, 3H, OCH_3), 3.65 (s, 6H, 2xOCH_3), 3.75 (s, 1H, H_3), 5.15 – 5.18 (m, 1H, H_4), 6.37 (s, 1H, ArH), 6.61 (s, 2H, ArH), 6.98 (s, 1H, ArH), 9.29 (s, 1H, OH), 9.56 (s, 1H, OH); ^{13}C NMR (100 MHz, DMSO-d_6) δ 14.64 (CH_3), 22.11 (CH_2), 43.51 (C_3), 49.06 (C_4), 55.58 (OCH_3), 55.65 (OCH_3), 60.08 (OCH_3), 93.95, 102.37, 112.87, 121.25, 128.25, 133.21, 134.17, 153.05, 154.53, 155.64 (ArC), 164.98 (C=O); HRMS: $C_{20}H_{23}NO_6Na$ requires 396.1423; found 396.1417 (M^++Na)

1-(2,3-Dihydrobenzo[b][1,4]dioxin-6-yl)-4-(5-ethyl-2,4-dihydroxyphenyl)-3-phenylazetidin-2-one (31) was obtained from 4-(2,4-bisbenzyloxy-5-ethyl-phenyl)-1-(2,3-dihydrobenzo[1,4]dioxin-6-yl)-3-phenyl-azetidin-2-one (**26**) as a yellow oil in 13.9% yield; purity: 99.4%; IR (KBr) ν_{max}: 1716.35 cm^{-1} (C=O, β-lactam); ^{1}H NMR (400 MHz, $CDCl_3$) δ 1.15 (t, 3H, CH_3), 2.48 – 2.54 (m, 2H, CH_2), 4.20 (s, 4H, OCH_2CH_2O), 4.46 (d, 1H, J=2 Hz, H_3), 5.12 (d, 1H, J=2 Hz, H_4), 6.28 (s, 1H, ArH), 6.74 (d, 1H, J=8.52 Hz, ArH), 6.88 (m, 1H, ArH), 6.99 – 7.01 (m, 2H, ArH), 7.29 – 7.37 (m, 5H, ArH); ^{13}C NMR (100 MHz, DMSO-d_6) δ 14.54 (CH_3), 22.18 (CH_2), 42.23 (C_3), 52.12 (C_4), 63.91 (CH_2), 64.17 (CH_2), 101.04, 102.46, 103.46, 107.36, 111.48, 111.72, 116.72, 116.95, 118.17, 118.51, 119.99, 121.98, 126.48, 127.53, 127.69, 127.87, 128.12, 128.20, 128.23, 128.52, 128.74, 131.76, 135.21, 138.54, 139.57, 141.15, 142.22, 152.84, 153.08, 153.94, 159.03, 160.15 (ArC), 169.72 (C=O); HRMS: $C_{25}H_{24}NO_5$ requires 418.1654; found 418.1656 (M^++H)

Biochemical Evaluation methods

Hsp90α fluorescent displacement assay: The assay is adapted from the method outlined by Howes[17, 35]. The components of the Hsp90 assay buffer are as follows: HEPES, pH 7.3 (20mM); Potassium chloride (50mM); Magnesium chloride (5mM); Na_2MoO_4 (20nM); 0.01% v/v NP40. The buffer is made up using distilled water. Directly before each use, 1mg bovine gamma globulin (per 10mL) and 3.085mg of DL-dithiothreitol (per 10mL) are added. Hsp90α recombinant human protein (Stressgen©) was used at a final protein concentration of 75nM and is diluted with assay buffer. FITC-geldanamycin (FITC-GA) is the fluorescent ligand used in this displacement assay at a final concentration of 5nM. 17-AAG is used as a positive control in the Hsp90 fluorescent displacement assay (reported IC_{50} value for binding in Hsp90 is 1.27μM[28]). For the assay, to each well is added: 69 μL buffer, 1 μL ligand, 25 μL receptor and 5 μL FITC-GA. The control rows consist of (two of each): buffer (75 μL) + receptor (25 μL); buffer (70 μL) + receptor (25 μL) + FITC-GA (5 μL); buffer (95 μL) + FITC-GA (5 μL) and vehicle controls as necessary. The assay is read on a fluorescent plate reader using excitation of 485/20 nM and emission 535/25 nM with polarisation. IC_{50} values were calculated using non-linear regression with a sigmoidal dose-response (variable slope) curve, using GraphPad Prism[50].

Antiproliferative MTT assay: All assays were performed in triplicate for the determination of mean values reported. The human breast tumour cell line MCF-7 was cultured in Eagles minimum essential medium at 37°C in a 95% O_2/5% CO_2 atmosphere with 10% fetal bovine serum, 2 mM L-glutamine and 100 μg/mL penicillin/streptomycin. The medium was supplemented with 1% non-essential amino acids. Cells were trypsinised and seeded at a density of 2.5 x 10^4 cells/mL in a 96-well plate and incubated at 37°C, 95%O_2/5% CO_2 atmosphere for 24 h. After this time they were treated with 2 μL volumes of test compound which had been pre-prepared as stock solutions in ethanol to furnish the concentration range of study, 1 nM–200 μM, and re-incubated for a further 72 h. Control wells contained the equivalent volume of the vehicle ethanol or DMSO (1% v/v). The culture medium was then removed and the cells washed with 100μL phosphate buffered saline (PBS) and 50 μL MTT (dissolved in PBS) added, to give a final concentration of 1 mg/mL MTT. Cells were incubated for 3

hours in darkness at 37°C. At this point solubilization was begun through the addition of 200 μL DMSO and the cells maintained at room temperature in darkness for 20 min to ensure thorough colour diffusion before reading the absorbance. The absorbance value of control cells (no added compound) was set to 100 % cell viability and from this graphs of absorbance versus cell density per well were prepared to assess cell viability using GraphPad Prism software[50].

Hsp90 Client Protein Degradation assay: MCF-7 cells were cultured as described for the antiproliferative assay. MCF-7 cells were seeded at a density of 1.0 x 10^6 cells / 25 cm^2 tissue culture flask (5ml Media) and left to adhere for 18 h prior to treatment. Cells were incubated with Vehicle (DMSO 0.5%) or compounds 17-AAG, **5**, **12**, and **18** at indicated concentrations for 24h. At the experimental endpoint, cells are tyrpsinised and washed twice in ice-cold PBS, before incubation on ice for 1h with 1 x Cell Lysis Ripa Buffer (50mM Tris-HCL (pH 7.4), 150 mM NaCL, 2 mM EDTA, 1% NP-40 (v/v), 0.1% SDS(w/v), 5 mM DTT and protease inhibiters). Cell debris was spun down at 10,000 x g and 4°C for 10 mins and supernatant was taken as whole cell lysate. Lysate protein concentrations were determined by way of a BCA protein assay (Thermo Scientific). Equal amount of proteins (25 μg) from each lysate were resolved on an 8% SDS-polyacrylamide gel and transferred to a PVDF membrane (Millipore) for Western blot analysis.

Estrogen receptor alpha protein expression levels were determined by probing with an ER-α mouse monoclonal antibody (Cell Signalling – 62A3). A mouse monoclonal antibody against β-Actin (Calbiochem – Ab-1) was used as a loading control.

Molecular modelling methods

PDB entry 1OSF[27] (a co-crystal structure of 17-dimethylaminoethylamino-17-demethoxygeldanamycin in complex with human Hsp90α) was used in the docking procedure due to correct docking of 131 Hsp90 actives as demonstrated previously by Knox et al[17]. Several binding site waters were retained in the docking process as they provide key interactions in stabilising the ligand in the active site. Addition of hydrogens for the receptor and waters was carried out using MOEv2007.09 and optimization using the Amber99 force-field ensuring all other atom positions remained fixed. Docking constraints were added such that all docked poses must have a H-bonding interaction with Asp93 to be considered successfully docked. Docking was performed using the

docking algorithm FRED (Fast Rigid Exhaustive Docking[51]) and scored with Chemgauss3. Subsequent refinement of all side-chains within 5Å of the docked pose was carried out using Szybki (http://www.eyesopen.com).

Acknowledgements

This work was supported through funding from the Trinity College IITAC research initiative (funded under the Irish Higher Education Authority's Programme for Research in Third Level Institutions (PRTLI)), Enterprise Ireland (EI), Science Foundation Ireland (SFI), and the Health Research Board (HRB), with additional support for computational facilities from the Wellcome Trust. A postgraduate research award from Trinity College is gratefully acknowledged (NMO'B).

Figure legends

Figure 1. Hsp90 binding compounds including geldanamycin **1a**, 17-AAG **1b**, 17-DMAG **1c**, radicicol **2**, pyrazole-based inhibitors **3a** and **3b**, purine-based inhibitor **3c**, dual tubulin-Hsp90 inhibitor **4** and proposed β-lactam based inhibitor **5**

Figure 2. Flexible alignment of pyrazole **3a** (green) and β-lactam **5** (coloured by atom; grey = carbon; red = oxygen; blue = nitrogen)

Figure 3. Docking of β-lactam **5** in the N-terminal of Hsp90α (PBD code: 1OSF[27]). Key interactions for binding are depicted. Colour key: Green = carbon; Red = oxygen; Blue = nitrogen; hydrogen bonds shown as dashed blue lines and π interactions as dashed green lines.

Figure 4. 2D representation of proposed binding interactions of β-lactam **5** with Hsp90

Figure 5. Imine **12** in the ATP-binding site of Hsp90 with selected residues for binding shown (PDB code: 1OSF[27]); Colour key: Green = carbon; Red = oxygen; Blue = nitrogen; hydrogen bonds shown as dashed blue lines and π interactions as dashed green lines.

Figure 6. 2D representation of binding interactions of imine **12** with the ATP-binding site of Hsp90

Figure 7. Dose response graph for β-lactam **5**, imine **12** and 17-AAG (**1b**) for binding to Hsp90α.

MCF-7 cells were seeded at a density of 2.5 x 10^4 cells per well in 96 well plates. The plates were left for 24 hours to allow the cells to adhere to the surface of the wells. A range of concentrations (0.01 nM-100 μM) of the compound were added in triplicate and the cells left for another 72 hours. Control wells contained the equivalent volume of the vehicle ethanol (1% v/v). An MTT assay was performed to determine the level of anti-proliferation. The values represent the mean ± S.E.M (error values) for three experiments performed in triplicate.

Figure 8. β-Lactam compounds 5, 12 & 18 induce Hsp90 client protein degradation

β-Lactam scaffold compounds **5**, **12** and **18** induced proteasomal degradation of Hsp90 client protein, Estrogen Receptor Alpha (ERα), in the ERα+ breast cancer cell line, MCF-7. MCF-7 cells were treated with indicated concentrations of **5**, **12** and **18** in figure (**A**) and (**B**). Cells were seeded at a density of 1.0 x 10^6 cells / 25 cm^2 tissue culture flasks (5 mL Media). Cells were treated with Vehicle control (**C** – DMSO (0.5%)), test compounds **5**, **12**, **18** and positive control **17-AAG** (1, 5 & 10μM) and left incubate for 24h. Whole cell lysates were prepared and ERα protein expression was analysed by SDS-PAGE and Western Blot analysis. Beta-actin was used as a protein loading control. Results are representative of three independent experiments.

Scheme and Table Legends

Scheme 1: Synthesis of imines **9-18**[a]

[a]Reagents and conditions: (a) DMF, $POCl_3$, 80°C; (b) $C_6H_5CH_2Br$, K_2CO_3, CH_3CN; (c) HTMA, CF_3COOH, 100°C, 30 min;(d) Ethanol, reflux, 3 h

Scheme 2: Synthesis of azetidin-2-ones **19-26**[a]

[a]Reagents and conditions: (a) Zinc, TMCS, anhydrous benzene, microwave. Only one enantiomer is illustrated.

Scheme 3: Synthesis of azetidin-2-ones **5, 27-30**[a]

[a]Reagents and conditions: (a) H_2, Pd/C, Ethanol:Ethyl acetate (1:1)**.** Only one enantiomer is illustrated.

Table 1. Antiproliferative and Hsp90-binding effects of β-lactams and imines

[a]MCF-7 IC_{50} values are half maximal concentrations required to inhibit the growth stimulation of MCF-7 cells. Values represent the mean ± S.E.M (error values x 10^{-6}) for three independent experiments performed in triplicate. [b]Hsp90α values after 24 hours using isolated human Hsp90α; 17-AAG is used as a positive control in the Hsp90 fluorescent displacement assay and the value obtained agrees with the reported IC_{50} value for binding of 17-AAG in Hsp90 of 1.27 μM[28].

References

1. Smith, J. R.; Workman, P., Targeting the cancer chaperone HSP90. *Drug Discovery Today: Therapeutic Strategies* **2007;** *4* (4) 219-227.
2. Powers, M. V.; Workman, P., Inhibitors of the heat shock response: Biology and pharmacology. *FEBS Lett.* **2007;** *581* (19) 3758-3769.
3. Prodromou, C.; Roe, S. M.; O'Brien, R.; Ladbury, J. E.; Piper, P. W.; Pearl, L. H., Identification and Structural Characterisation of the ATP/ADP-binding site in the Hsp90 Molecular Chaperone. *Cell* **1997;** *90* 65-75.
4. Whitesell, L.; Mimnaugh, E. G.; De Costa, B.; Myers, C. E.; Neckers, L. M., Inhibition of heat shock protein HSP90-pp60v-src heteroprotein complex formation by benzoquinone ansamycins: essential role for stress proteins in oncogenic transformation. *Proc. Natl. Acad. Sci. U.S.A.* **1994;** *91* (18) 8324-8328.
5. Schnur, R. C.; Corman, M. L.; Gallaschun, R. J.; Cooper, B. A.; Dee, M. F.; Doty, J. L.; Muzzi, M. L.; Moyer, J. D.; DiOrio, C. I., Inhibition of the oncogene product p185erbB-2 in vitro and in vivo by geldanamycin and dihydrogeldanamycin derivatives. *J. Med. Chem.* **1995;** *38* (19) 3806-3812.
6. Schulte, T. W.; Akinaga, S.; Soga, S.; Sullivan, W.; Stensgard, B.; Toft, D.; Neckers, L. M., Antibiotic radicicol binds to the N-terminal domain of Hsp90 and shares important biologic activities with geldanamycin. *Cell Stress Chaperones* **1998;** *3* (2) 100-108.
7. Roe, S. M.; Prodromou, C.; O'Brien, R.; Ladbury, J. E.; Piper, P. W.; Pearl, L. H., Structural Basis for Inhibition of the Hsp90 Molecular Chaperone by the Antitumor Antibiotics Radicicol and Geldanamycin. *J. Med. Chem.* **1999;** *42* (2) 260-266.
8. Stebbins, C. E.; Russo, A. A.; Schneider, C.; Rosen, N.; Hartl, F. U.; Pavletich, N. P., Crystal Structure of an Hsp90 Geldanamycin Complex: Targeting of a Protein Chaperone by an Antitumor Agent. *Cell* **1997;** *89* (2) 239-250.
9. Agatsuma, T.; Ogawa, H.; Akasaka, K.; Asai, A.; Yamashita, Y.; Mizukami, T.; Akinaga, S.; Saitoh, Y., Halohydrin and Oxime Derivatives of Radicicol: Synthesis and Antitumor Activities. *Bioorg. Med. Chem.* **2002;** *10* (11) 3445-3454.
10. Janin, Y. L., Heat Shock Protein 90 Inhibitors. A Text Book Example of Medicinal Chemistry? *J. Med. Chem.* **2005;** *48* (24) 7503-7512.
11. Kreusch, A.; Han, S.; Brinker, A.; Zhou, V.; Choi, H.-s.; He, Y.; Lesley, S. A.; Caldwell, J.; Gu, X.-j., Crystal structures of human HSP90[alpha]-complexed with dihydroxyphenylpyrazoles. *Bioorg. Med. Chem. Lett.* **2005;** *15* (5) 1475-1478.
12. Chiosis, G.; Vilenchik, M.; Kim, J.; Solit, D., Hsp90: the vulnerable chaperone. *Drug Discovery Today* **2004;** *9* (20) 881-888.
13. McDonald, E.; Workman, P.; Jones, K., Inhibitors of the HSP90 Molecular Chaperone: Attacking the Master Regulator in Cancer. *Current Topics in Medicinal Chemistry* **2006;** *6* (11) 1091-1107.
14. McDonald, E.; Jones, K.; Brough, P. A.; Drysdale, M. J.; Workman, P., Discovery and Development of Pyrazole-Scaffold Hsp90 Inhibitors. *Current Topics in Medicinal Chemistry* **2006;** *6* (11) 1193-1203.
15. Cheung, K.-M. J.; Matthews, T. P.; James, K.; Rowlands, M. G.; Boxall, K. J.; Sharp, S. Y.; Maloney, A.; Roe, S. M.; Prodromou, C.; Pearl, L. H.; Aherne, G. W.; McDonald, E.; Workman, P., The identification, synthesis, protein crystal structure and in vitro biochemical evaluation of a new 3,4-diarylpyrazole class of Hsp90 inhibitors. *Bioorganic & Medicinal Chemistry Letters* **2005;** *15* (14) 3338-3343.
16. Wright, L.; Barril, X.; Dymock, B.; Sheridan, L.; Surgenor, A.; Beswick, M.; Drysdale, M.; Collier, A.; Massey, A.; Davies, N.; Fink, A.; Fromont, C.; Aherne, W.; Boxall, K.; Sharp, S.;

Workman, P.; Hubbard, R. E., Structure-Activity Relationships in Purine-Based Inhibitor Binding to HSP90 Isoforms. *Chemistry & Biology* **2004;** *11* (6) 775-785.

17. Knox, A. J. S.; Price, T.; Pawlak, M.; Golfis, G.; Flood, C. T.; Fayne, D.; Williams, D. C.; Meegan, M. J.; Lloyd, D. G., Integration of Ligand and Structure-Based Virtual Screening for the Identification of the First Dual Targeting Agent for Heat Shock Protein 90 (Hsp90) and Tubulin. *J. Med. Chem.* **2009;** *52* (8) 2177-2180.

18. Biamonte, M. A.; Van de Water, R.; Arndt, J. W.; Scannevin, R. H.; Perret, D.; Lee, W.-C., Heat Shock Protein 90: Inhibitors in Clinical Trials. *J. Med. Chem.* **2009;** *53* (1) 3-17.

19. www.clinicaltrials.gov (Accessed 3rd March 2011),

20. Bao, R.; Lai, C.-J.; Qu, H.; Wang, D.; Yin, L.; Zifcak, B.; Atoyan, R.; Wang, J.; Samson, M.; Forrester, J.; DellaRocca, S.; Xu, G.-X.; Tao, X.; Zhai, H.-X.; Cai, X.; Qian, C., CUDC-305, a Novel Synthetic HSP90 Inhibitor with Unique Pharmacologic Properties for Cancer Therapy. *Clinical Cancer Research* **2009;** *15* (12) 4046-4057.

21. Woodhead, A. J.; Angove, H.; Carr, M. G.; Chessari, G.; Congreve, M.; Coyle, J. E.; Cosme, J.; Graham, B.; Day, P. J.; Downham, R.; Fazal, L.; Feltell, R.; Figueroa, E.; Frederickson, M.; Lewis, J.; McMenamin, R.; Murray, C. W.; O'Brien, M. A.; Parra, L.; Patel, S.; Phillips, T.; Rees, D. C.; Rich, S.; Smith, D.-M.; Trewartha, G.; Vinkovic, M.; Williams, B.; Woolford, A. J. A., Discovery of (2,4-Dihydroxy-5-isopropylphenyl)-[5-(4-methylpiperazin-1-ylmethyl)-1,3-dihydroisoindol-2-yl]methanone (AT13387), a Novel Inhibitor of the Molecular Chaperone Hsp90 by Fragment Based Drug Design. *Journal of Medicinal Chemistry* **2010;** *53* (16) 5956-5969.

22. Nakashima, T.; Ishii, T.; Tagaya, H.; Seike, T.; Nakagawa, H.; Kanda, Y.; Akinaga, S.; Soga, S.; Shiotsu, Y., New Molecular and Biological Mechanism of Antitumor Activities of KW-2478, a Novel Nonansamycin Heat Shock Protein 90 Inhibitor, in Multiple Myeloma Cells. *Clinical Cancer Research* **2010;** *16* (10) 2792-2802.

23. Georg, G. I., *The Organic Chemistry of Beta-Lactams*. VCH Publishers, Inc.: New York and Cambridge, **1992**.

24. Clader, J. W.; Burnett, D. A.; Caplen, M. A.; Domalski, M. S.; Dugar, S.; Vaccaro, W.; Sher, R.; Browne, M. E.; Zhao, H.; Burrier, R. E.; Salisbury, B.; Davis, H. R., Jr., 2-Azetidinone cholesterol absorption inhibitors: structure-activity relationships on the heterocyclic nucleus. *J. Med. Chem.* **1996;** *39* (19) 3684-3693.

25. O'Boyle, N. M.; Carr, M.; Greene, L. M.; Bergin, O.; Nathwani, S. M.; McCabe, T.; Lloyd, D. G.; Zisterer, D. M.; Meegan, M. J., Synthesis and Evaluation of Azetidinone Analogues of Combretastatin A-4 as Tubulin Targeting Agents. *Journal of Medicinal Chemistry* **2010;** *53* (24) 8569-8584.

26. Carr, M.; Greene, L. M.; Knox, A. J. S.; Lloyd, D. G.; Zisterer, D. M.; Meegan, M. J., Lead identification of conformationally restricted beta-lactam type combretastatin analogues: synthesis, antiproliferative activity and tubulin targeting effects. *European Journal of Medicinal Chemistry* **2010;** *45* (12) 5752-5766.

27. Jez, J. M.; Chen, J. C. H.; Rastelli, G.; Stroud, R. M.; Santi, D. V., Crystal Structure and Molecular Modeling of 17-DMAG in Complex with Human Hsp90. *Chem. Biol.* **2003;** *10* (4) 361-368.

28. Dymock, B. W.; Barril, X.; Brough, P. A.; Cansfield, J. E.; Massey, A.; McDonald, E.; Hubbard, R. E.; Surgenor, A.; Roughley, S. D.; Webb, P.; Workman, P.; Wright, L.; Drysdale, M. J., Novel, Potent Small-Molecule Inhibitors of the Molecular Chaperone Hsp90 Discovered through Structure-Based Design. *Journal of Medicinal Chemistry* **2005;** *48* (13) 4212-4215.

29. Clark, A. M.; Labute, P., 2D Depiction of Protein-Ligand Complexes. *J. Chem. Inf. Model.* **2007;** *47* (5) 1933-1944.

30. Chiosis, G.; Lucas, B.; Huezo, H.; Solit, D.; Basso, A.; Rosen, N., Development of Purine-Scaffold Small Molecule Inhibitors of Hsp90. *Curr. Cancer Drug Targets* **2003;** *3* (5) 371.

31. Shen, G.; Wang, M.; Welch, T. R.; Blagg, B. S. J., Design, Synthesis, and Structure Activity Relationships for Chimeric Inhibitors of Hsp90. *J. Org. Chem.* **2006;** *71* (20) 7618-7631.

32. Duff, J. C.; Bills, E. J., 273. Reactions between hexamethylenetetramine and phenolic compounds. Part I. A new method for the preparation of 3- and 5-aldehydosalicylic acids. *J. Chem. Soc.* **1932;** 1987 - 1988.

33. Duff, J. C.; Bills, E. J., 282. Reactions between hexamethylenetetramine and phenolic compounds. Part II. Formation of phenolic aldehydes. Distinctive behaviour of p-nitrophenol. *J. Chem. Soc.* **1934;** 1305 - 1308.

34. Duff, J. C., 96. A new general method for the preparation of o-hydroxyaldehydes from phenols and hexamethylenetetramine. *J. Chem. Soc.* **1941;** 547 - 550.

35. Howes, R.; Barril, X.; Dymock, B. W.; Grant, K.; Northfield, C. J.; Robertson, A. G. S.; Surgenor, A.; Wayne, J.; Wright, L.; James, K.; Matthews, T.; Cheung, K. M.; McDonald, E.; Workman, P.; Drysdale, M. J., A fluorescence polarization assay for inhibitors of Hsp90. *Analytical Biochemistry* **2006;** *350* (2) 202-213.

36. Kyle Hadden, M.; Lubbers, D. J.; Blagg, B. S. J., Geldanamycin, Radicicol, and Chimeric Inhibitors of the Hsp90 Nterminal ATP Binding Site. *Curr. Top. Med. Chem.* **2006;** *6* (11) 1173-1182.

37. Barril, X.; Beswick, M. C.; Collier, A.; Drysdale, M. J.; Dymock, B. W.; Fink, A.; Grant, K.; Howes, R.; Jordan, A. M.; Massey, A.; Surgenor, A.; Wayne, J.; Workman, P.; Wright, L., 4-Amino derivatives of the Hsp90 inhibitor CCT018159. *Bioorganic & Medicinal Chemistry Letters* **2006;** *16* (9) 2543-2548.

38. Brandt, G. E. L.; Schmidt, M. D.; Prisinzano, T. E.; Blagg, B. S. J., Gedunin, a Novel Hsp90 Inhibitor: Semisynthesis of Derivatives and Preliminary Structure-Activity Relationships. *J. Med. Chem.* **2008;** *51* (20) 6495-6502.

39. Barta, T. E.; Veal, J. M.; Rice, J. W.; Partridge, J. M.; Fadden, R. P.; Ma, W.; Jenks, M.; Geng, L.; Hanson, G. J.; Huang, K. H.; Barabasz, A. F.; Foley, B. E.; Otto, J.; Hall, S. E., Discovery of benzamide tetrahydro-4H-carbazol-4-ones as novel small molecule inhibitors of Hsp90. *Bioorg. Med. Chem. Lett.* **2008;** *18* (12) 3517-3521.

40. Chiosis, G.; Lucas, B.; Shtil, A.; Huezo, H.; Rosen, N., Development of a Purine-Scaffold Novel Class of Hsp90 Binders that Inhibit the Proliferation of Cancer Cells and Induce the Degradation of Her2 Tyrosine Kinase. *Bioorg. Med. Chem.* **2002;** *10* (11) 3555-3564.

41. Muranaka, K.; Sano, A.; Ichikawa, S.; Matsuda, A., Synthesis of Hsp90 inhibitor dimers as potential antitumor agents. *Bioorg. Med. Chem.* **2008;** *16* (11) 5862-5870.

42. Radanyi, C.; Le Bras, G.; Messaoudi, S.; Bouclier, C.; Peyrat, J.-F.; Brion, J.-D.; Marsaud, V.; Renoir, J.-M.; Alami, M., Synthesis and biological activity of simplified denoviose-coumarins related to novobiocin as potent inhibitors of heat-shock protein 90 (hsp90). *Bioorganic & Medicinal Chemistry Letters* **2008;** *18* (7) 2495-2498.

43. Ganesh, T.; Min, J.; Thepchatri, P.; Du, Y.; Li, L.; Lewis, I.; Wilson, L.; Fu, H.; Chiosis, G.; Dingledine, R.; Liotta, D.; Snyder, J. P.; Sun, A., Discovery of aminoquinolines as a new class of potent inhibitors of heat shock protein 90 (Hsp90): Synthesis, biology, and molecular modeling. *Bioorg. Med. Chem.* **2008;** *16* (14) 6903-6910.

44. Ge, J.; Normant, E.; Porter, J. R.; Ali, J. A.; Dembski, M. S.; Gao, Y.; Georges, A. T.; Grenier, L.; Pak, R. H.; Patterson, J.; Sydor, J. R.; Tibbitts, T. T.; Tong, J. K.; Adams, J.; Palombella, V. J., Design, Synthesis, and Biological Evaluation of Hydroquinone Derivatives of

17-Amino-17-demethoxygeldanamycin as Potent, Water-Soluble Inhibitors of Hsp90. *Journal of Medicinal Chemistry* **2006;** *49* (15) 4606-4615.

45. Brough, P. A.; Barril, X.; Borgognoni, J.; Chene, P.; Davies, N. G. M.; Davis, B.; Drysdale, M. J.; Dymock, B.; Eccles, S. A.; Garcia-Echeverria, C.; Fromont, C.; Hayes, A.; Hubbard, R. E.; Jordan, A. M.; Jensen, M. R.; Massey, A.; Merrett, A.; Padfield, A.; Parsons, R.; Radimerski, T.; Raynaud, F. I.; Robertson, A.; Roughley, S. D.; Schoepfer, J.; Simmonite, H.; Sharp, S. Y.; Surgenor, A.; Valenti, M.; Walls, S.; Webb, P.; Wood, M.; Workman, P.; Wright, L., Combining Hit Identification Strategies: Fragment-Based and in Silico Approaches to Orally Active 2-Aminothieno[2,3-d]pyrimidine Inhibitors of the Hsp90 Molecular Chaperone. *Journal of Medicinal Chemistry* **2009;** *52* (15) 4794-4809.

46. Kuduk, S. D.; Harris, C. R.; Zheng, F. F.; Sepp-Lorenzino, L.; Ouerfelli, Q.; Rosen, N.; Danishefsky, S. J., Synthesis and evaluation of geldanamycin-testosterone hybrids. *Bioorganic & Medicinal Chemistry Letters* **2000;** *10* (11) 1303-1306.

47. Le Bras, G.; Radanyi, C.; Peyrat, J. F.; Brion, J. D.; Alami, M.; Marsaud, V.; Stella, B.; Renoir, J. M., New novobiocin analogues as antiproliferative agents in breast cancer cells and potential inhibitors of heat shock protein 90. *J. Med. Chem.* **2007;** *50* 6189-6200.

48. Robinson, R.; Shah, R. C., Some homologs of resorcinol *J. Chem. Soc.* **1934;** 1491-1498.

49. Elin, E. A.; De Macedo, B. F.; Onoprienko, V. V.; Osokina, N. E.; Tikhomirova, O. B., Synthesis of argiopine *Bioorg. Khim.* **1988;** *14* (5) 704-706.

50. *GraphPad Prism version 4.00 for Windows, GraphPad Software, SanDiego California USA, www.graphpad.com*, 2009.

51. Fulda, S.; Galluzzi, L.; Kroemer, G., Targeting mitochondria for cancer therapy. *Nat Rev Drug Discov* **2010;** *9* (6) 447-464.

Compound	IC_{50} MCF-7 (μM)[a]	IC_{50} Hsp90α (μM)[b]
5	48 ± 2	5.6 ± 3.6
12	>100	14.5 ± 2.6
18	>100	22.1 ± 1.4
19	54 ± 26	> 200
20	53 ± 3	> 200
27	23 ± 11	> 200
28	52 ± 6	> 200
29	31 ± 18	> 200
30	31 ± 8	> 200
31	>100	> 200
17-AAG	0.09[40]	1.19

Figure 1

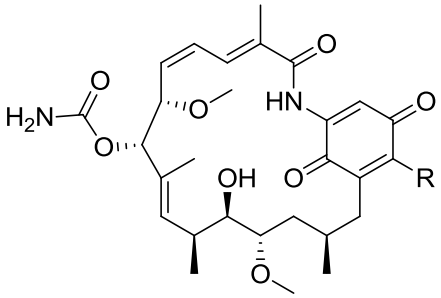

1a: R=OCH_3
1b: R=$NHCH_2CHCH_3$
1c: R=$NHCH_2CH_2N(CH_3)_2$

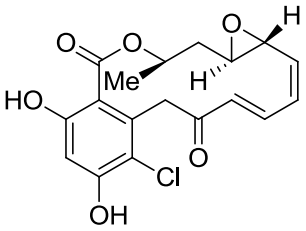

2

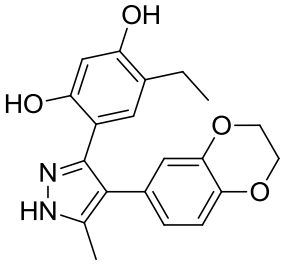

3a

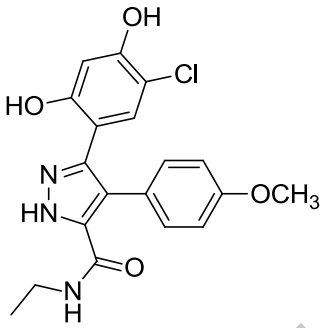

3b

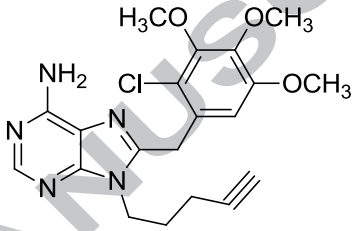

3c

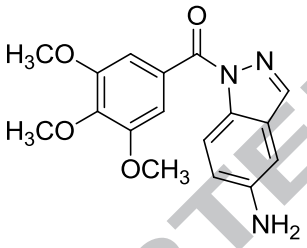

4

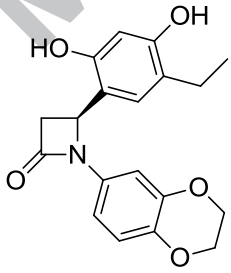

5

Figure 2

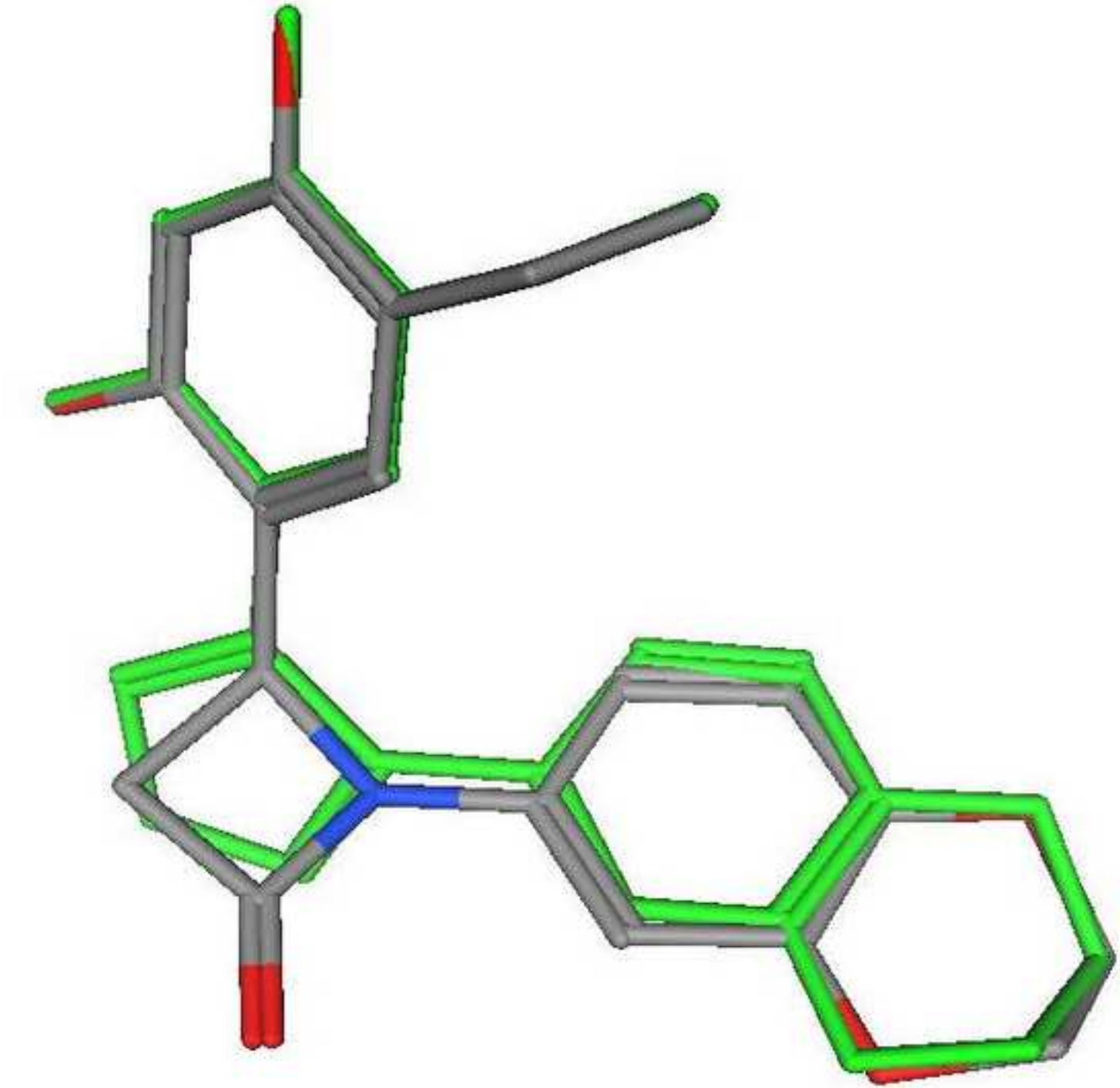

Figure 3

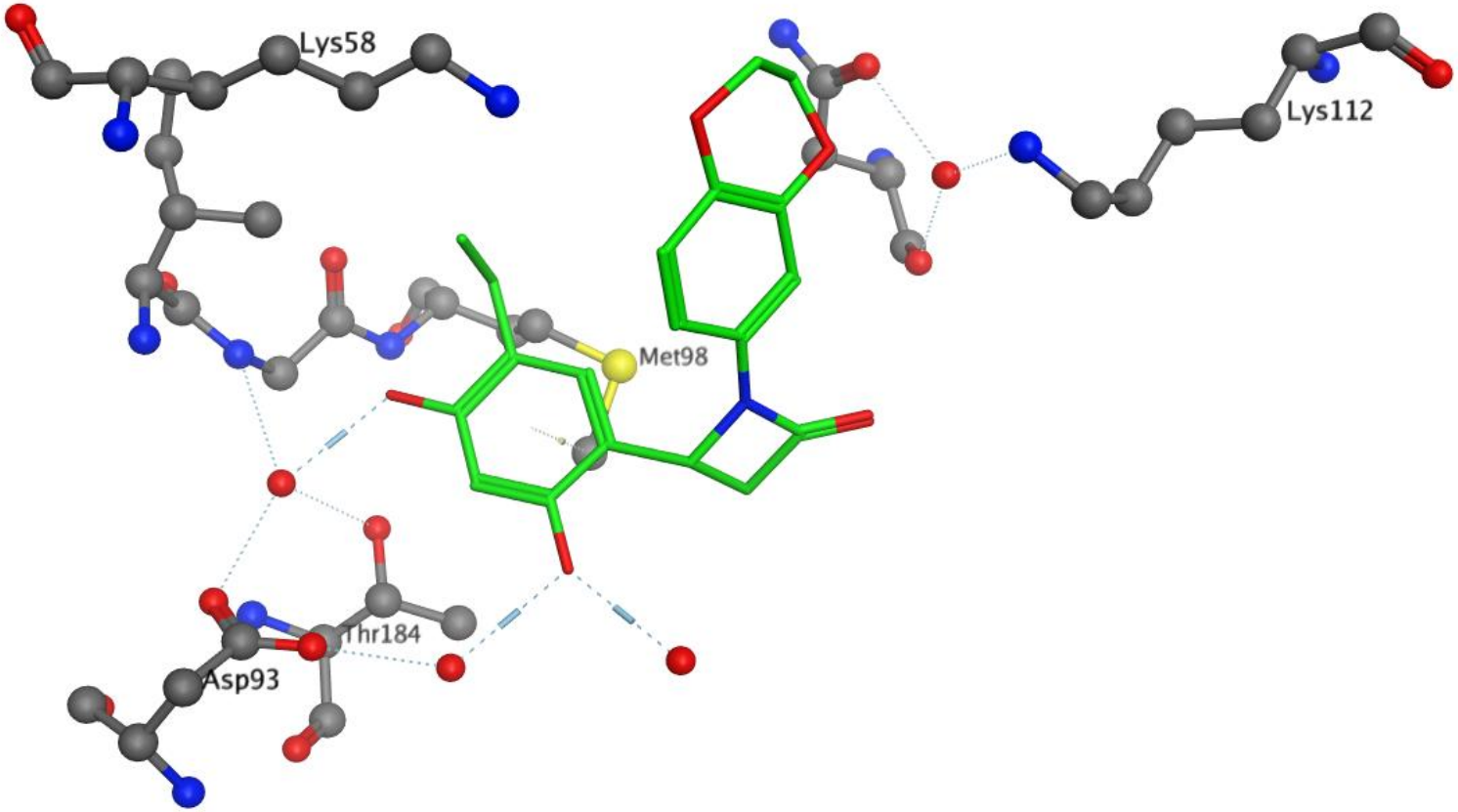

Figure 4

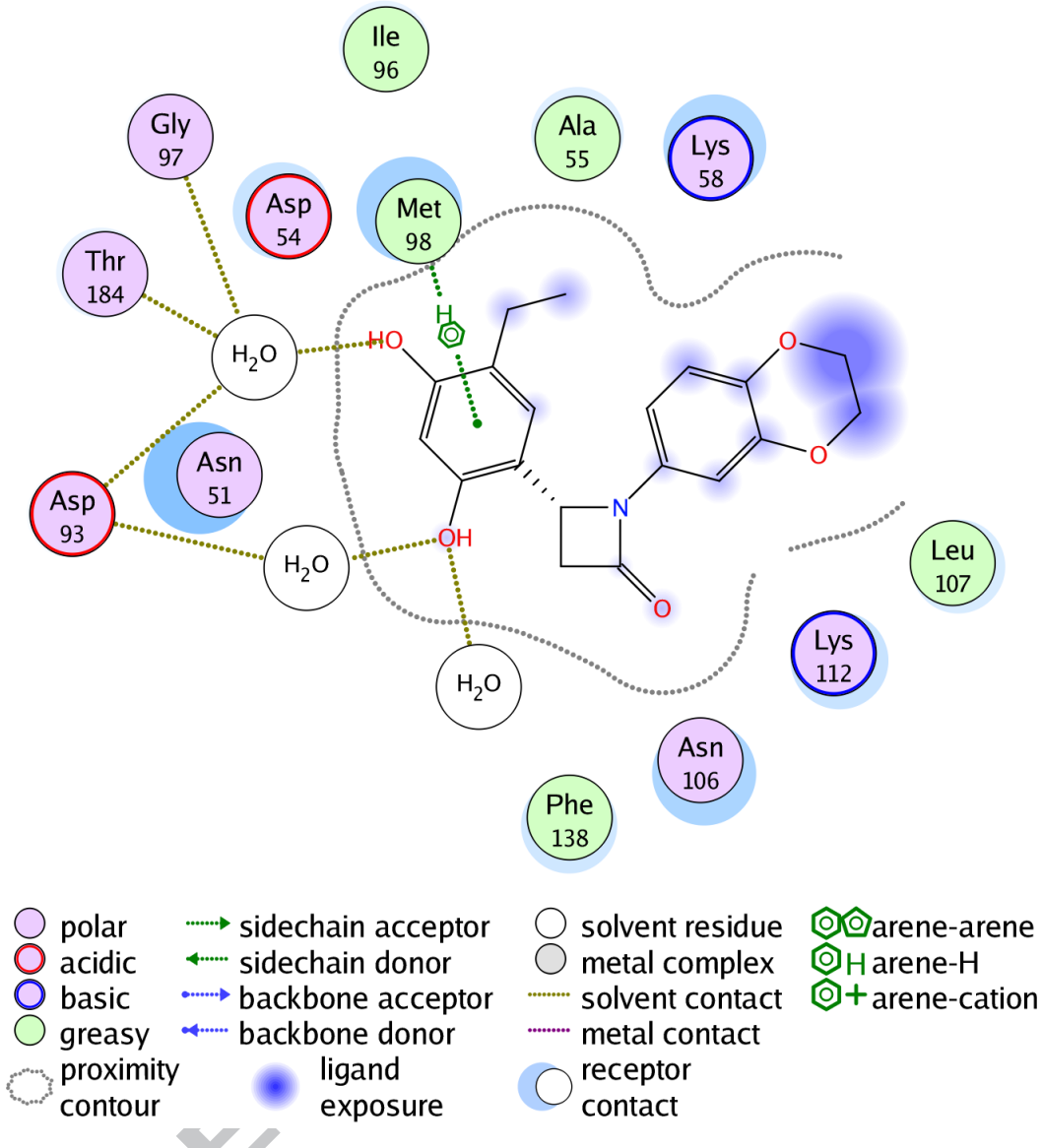

Figure 5

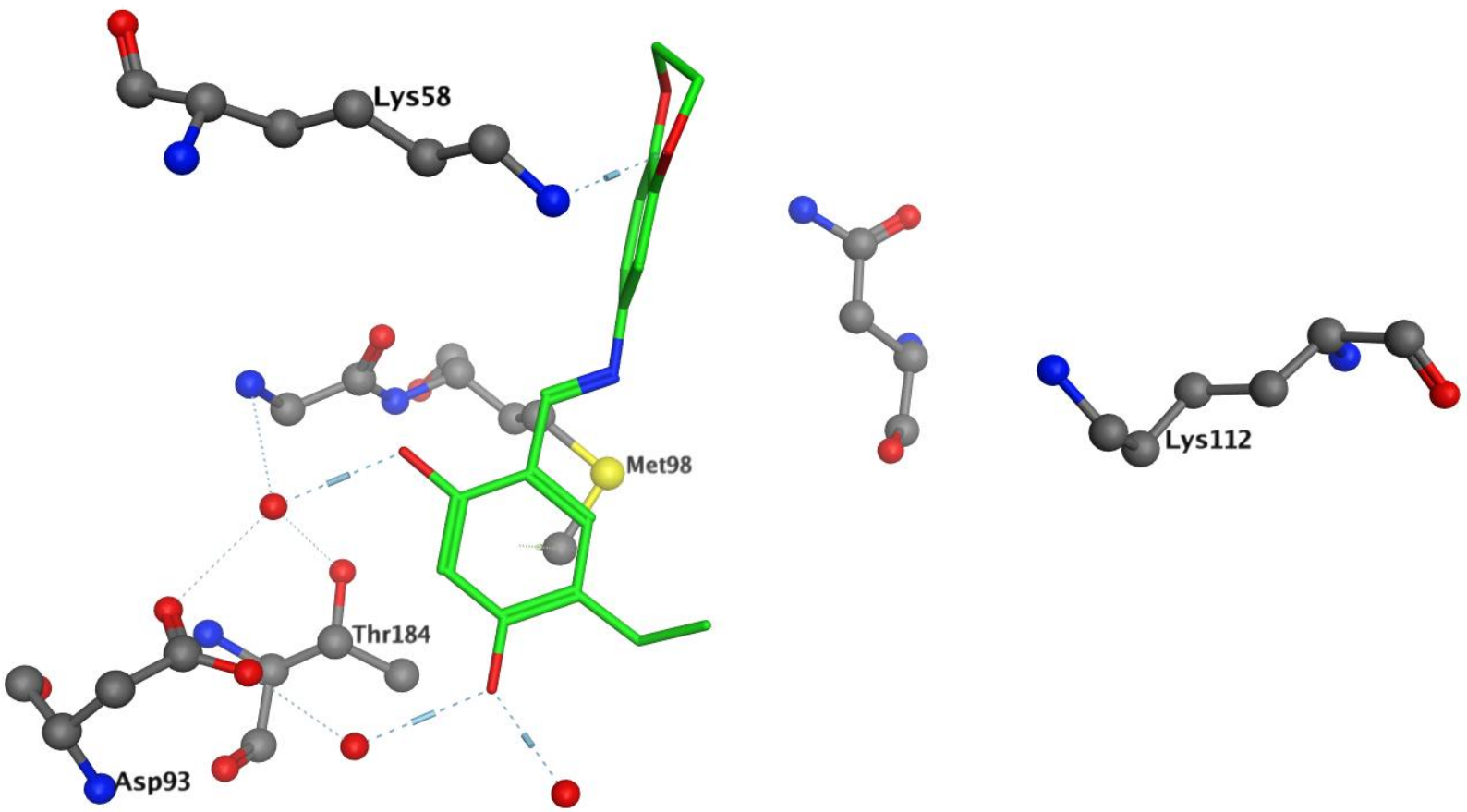

Figure 6

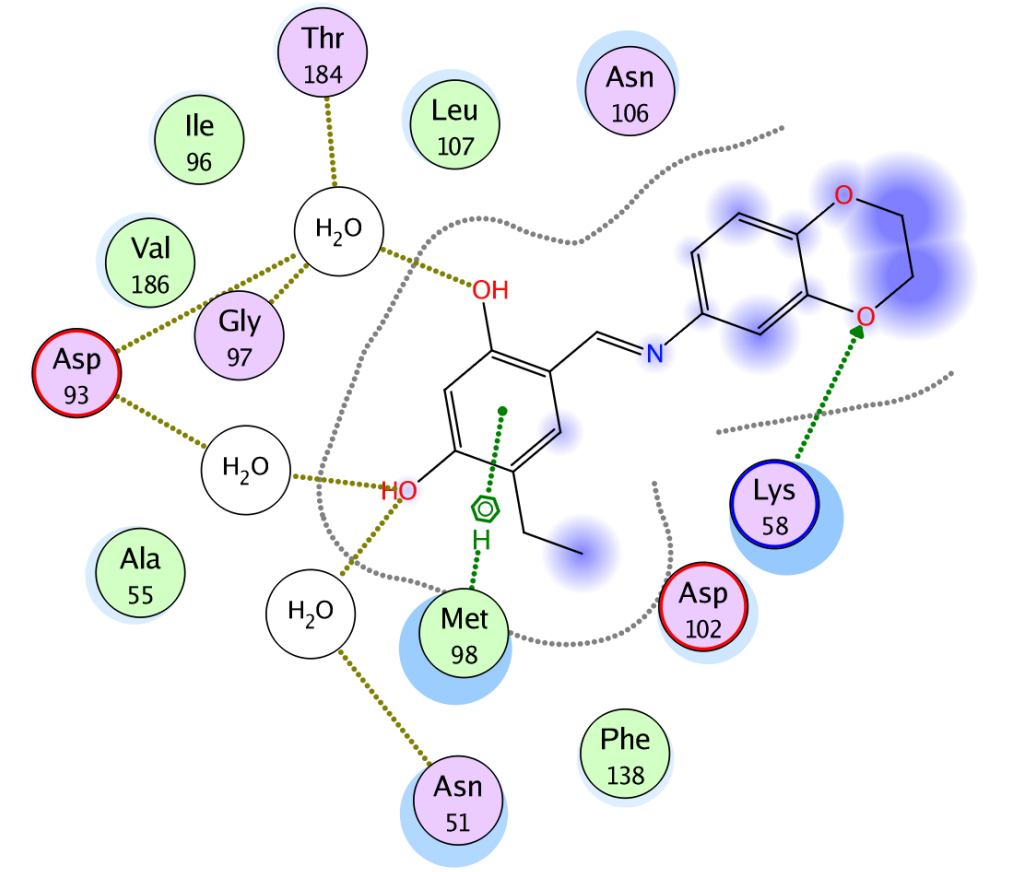

Figure 7

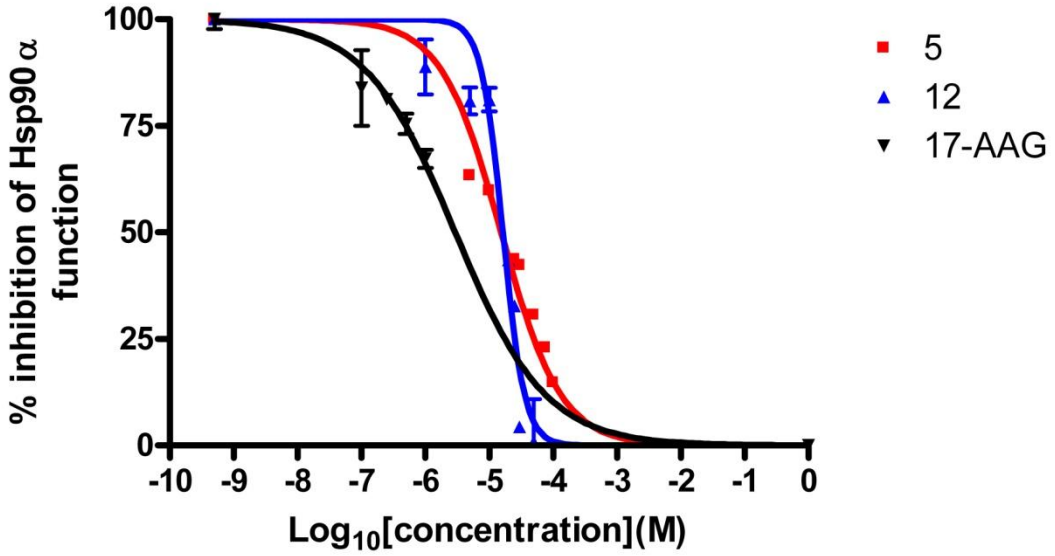

Figure 8

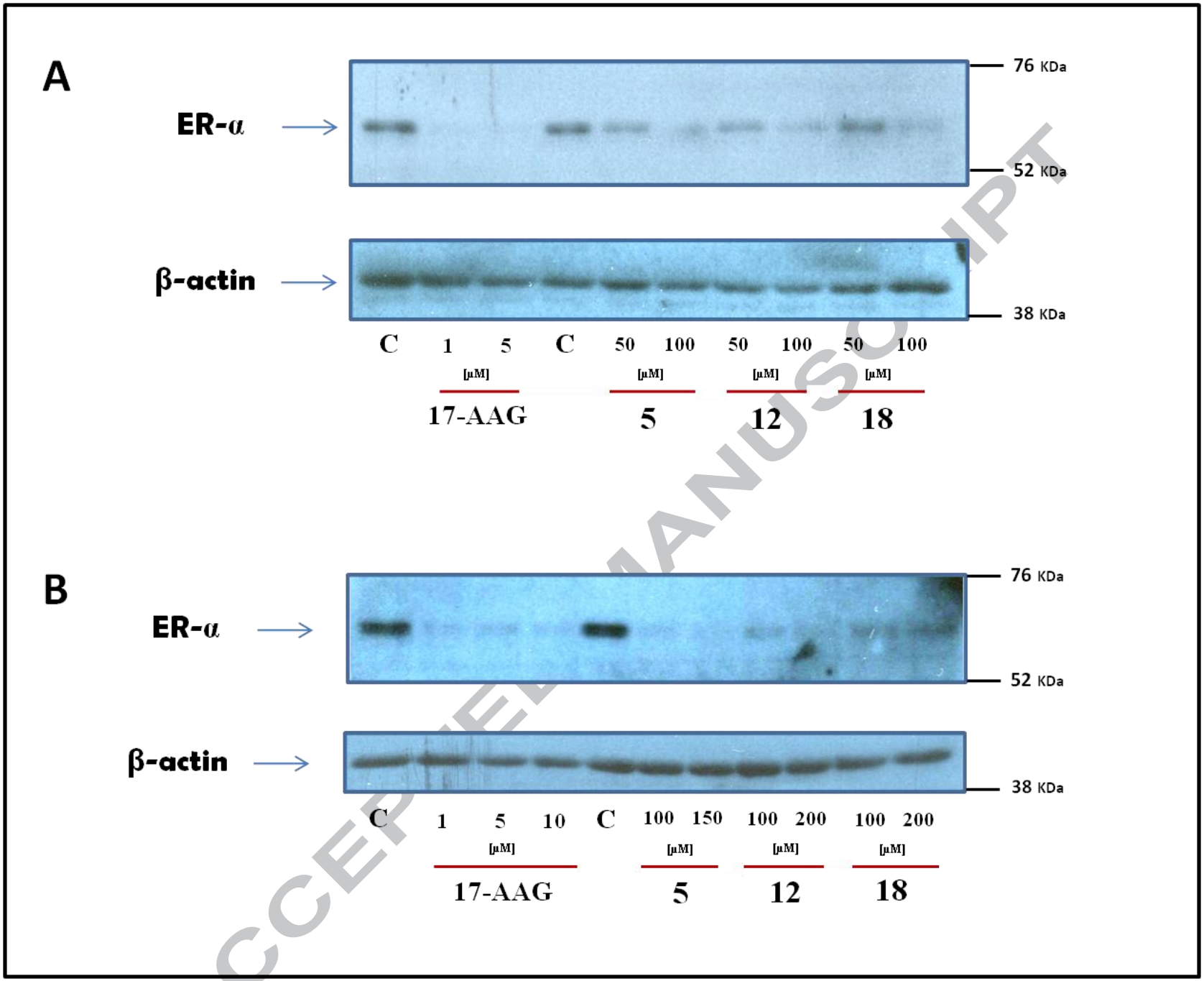

Scheme 1

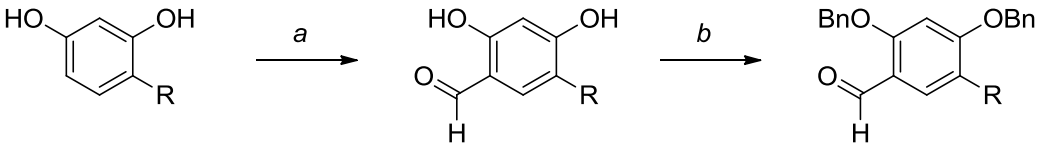

6a: R = H
6b: R = CH_2CH_3
6c: R = Cl

7a: R = H
7b: R = CH_2CH_3

8a R = H
8b R = CH_2CH_3

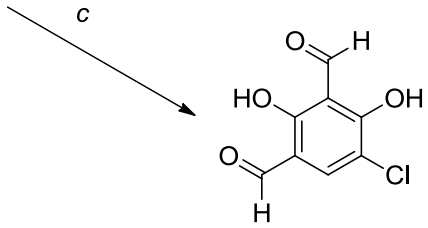

7c

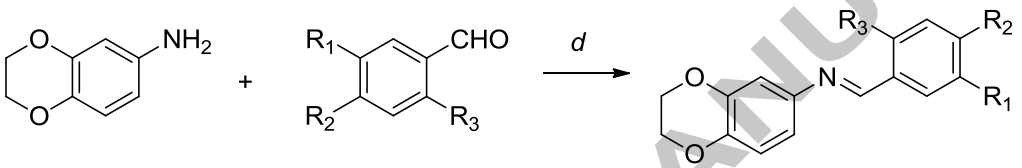

R=H unless otherwise indicated
9: $R_2=R_3=OCH_3$
10: $R_1=R_3=OCH_3$
11: $R_2=R_3=OH$
12: $R_1=C_2H_5$; $R_2=R_3=OH$
13: $R_2=R_3=OCH_2C_6H_5$
14: $R_1=C_2H_5$; $R_2=R_3=OCH_2C_6H_5$

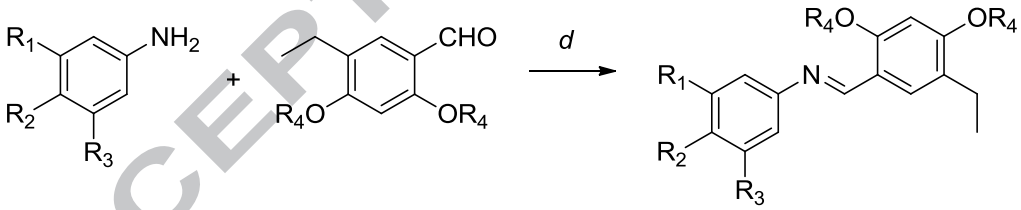

R=H unless otherwise indicated
15: $R_1=R_2=$ -OCH_2O-; $R_4=CH_2C_6H_5$
16: $R_1=R_2=R_3=OCH_3$; $R_4=CH_2C_6H_5$
17: $R_2=OCH_3$; $R_4=CH_2C_6H_5$
18: $R_1=R_2=$ -OCH_2O-

Scheme 2

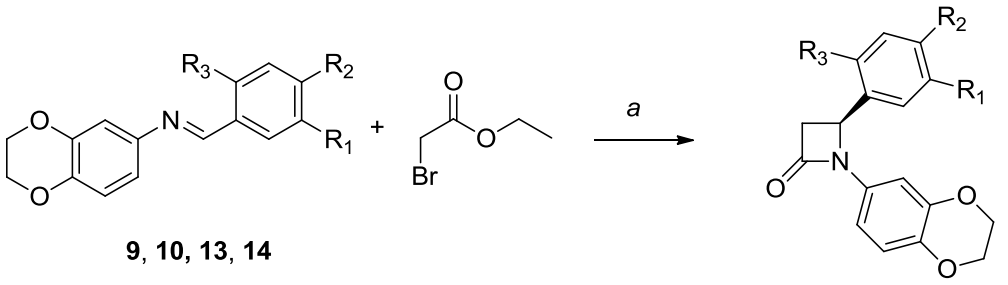

9, **10, 13**, **14**

R=H unless otherwise indicated
19: $R_1=R_3=OCH_3$
20: $R_2=R_3=OCH_3$
21: $R_2=R_3=OCH_2C_6H_5$
22: $R_1=C_2H_5$; $R_2=R_3=OCH_2C_6H_5$

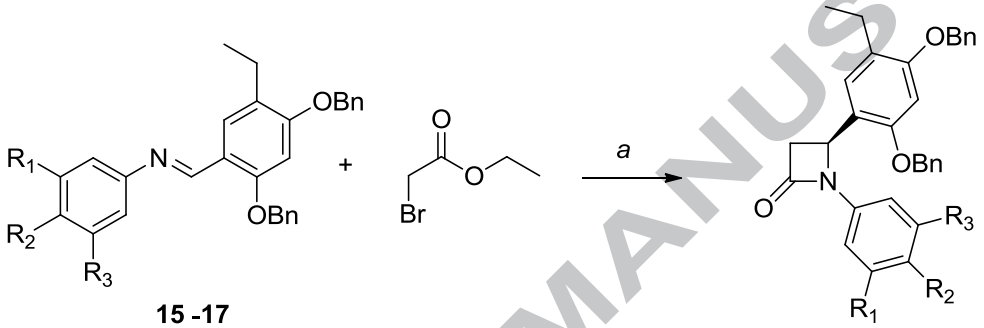

15 -17

R=H unless otherwise indicated
23: $R_2=OCH_3$
24: $R_1=R_2=$ -OCH_2O-
25: $R_1=R_2=R_3=OCH_3$

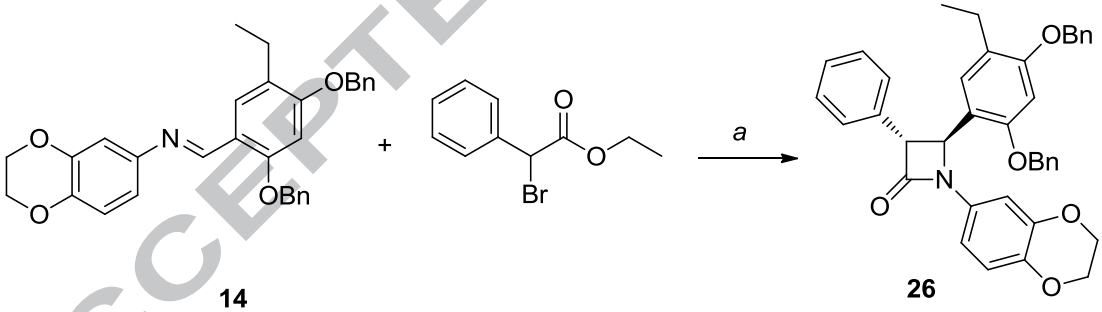

14

26

Scheme 3

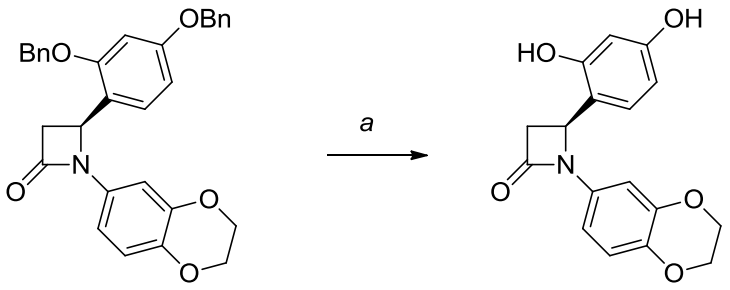

21 **27**

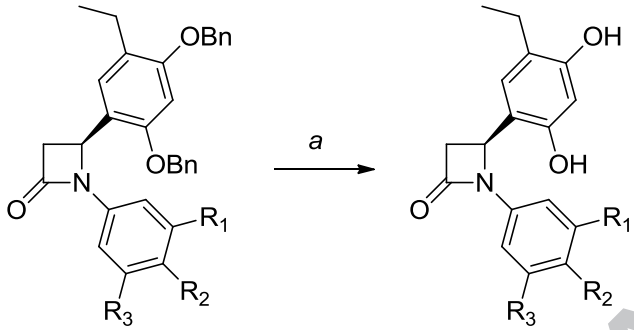

22 - 25

5: R_1=R_2= -OCH_2CH_2O-
28: R_2=OCH_3
29: R_1=R_2= -OCH_2O-
30: R_1=R_2=R_3=OCH_3

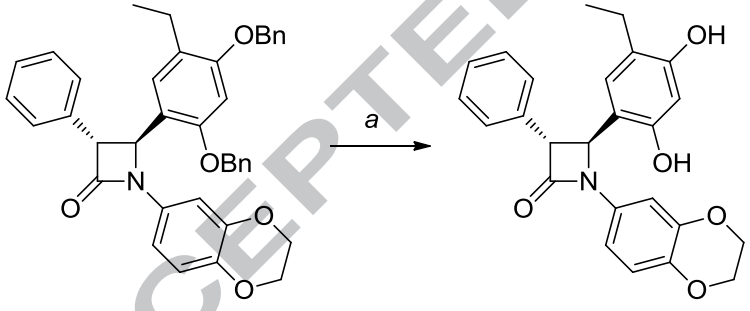

26 **31**

Graphical Abstract

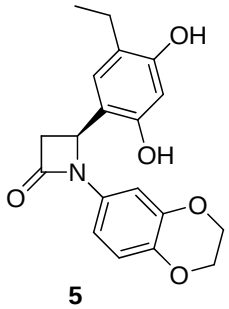

5

$Hsp90_{alpha}$ IC_{50} = 5.6 uM

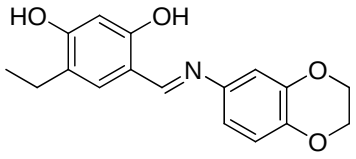

12

$Hsp90_{alpha}$ IC_{50} = 14.5 uM